Redox Biology 23 (2019) 101098

Contents lists available at ScienceDirect

Redox Biology

journal homepage: www.elsevier.com/locate/redox

Research Paper

Vimentin disruption by lipoxidation and electrophiles: Role of the cysteine residue and filament dynamics

Andreia Mónico[a], Sofia Duarte[a], María A. Pajares[a,b], Dolores Pérez-Sala[a,*]

[a] Department of Structural and Chemical Biology, Centro de Investigaciones Biológicas (CSIC), Ramiro de Maeztu 9, 28040 Madrid, Spain
[b] Molecular Hepatology Group, Instituto de Investigación Sanitaria del Hospital Universitario La Paz (IdiPAZ), Paseo de la Castellana 261, 28046 Madrid, Spain

ARTICLE INFO

Keywords:
Vimentin
Lipoxidation
HNE
Cyclopentenone prostaglandins
Intermediate filaments
Vimentin filament morphology and dynamics
Vimentin oxidation

ABSTRACT

The intermediate filament protein vimentin constitutes a critical sensor for electrophilic and oxidative stress, which induce extensive reorganization of the vimentin cytoskeletal network. Here, we have investigated the mechanisms underlying these effects. In vitro, electrophilic lipids, including 15-deoxy-$\Delta^{12,14}$-prostaglandin J_2 (15d-PGJ_2) and 4-hydroxynonenal (HNE), directly bind to vimentin, whereas the oxidant diamide induces disulfide bond formation. Mutation of the single vimentin cysteine residue (Cys328) blunts disulfide formation and reduces lipoxidation by 15d-PGJ_2, but not HNE. Preincubation with these agents differentially hinders NaCl-induced filament formation by wild-type vimentin, with effects ranging from delayed elongation and increased filament diameter to severe impairment of assembly or aggregation. Conversely, the morphology of vimentin Cys328Ser filaments is mildly or not affected. Interestingly, preformed vimentin filaments are more resistant to electrophile-induced disruption, although chemical modification is not diminished, showing that vimentin (lip) oxidation prior to assembly is more deleterious. In cells, electrophiles, particularly diamide, induce a fast and drastic disruption of existing filaments, which requires the presence of Cys328. As the cellular vimentin network is under continuous remodeling, we hypothesized that vimentin exchange on filaments would be necessary for diamide-induced disruption. We confirmed that strategies reducing vimentin dynamics, as monitored by FRAP, including cysteine crosslinking and ATP synthesis inhibition, prevent diamide effect. In turn, phosphorylation may promote vimentin disassembly. Indeed, treatment with the phosphatase inhibitor calyculin A to prevent dephosphorylation intensifies electrophile-induced wild-type vimentin filament disruption. However, whereas a phosphorylation-deficient vimentin mutant is only partially protected from disorganization, Cys328Ser vimentin is virtually resistant, even in the presence of calyculin A. Together, these results indicate that modification of Cys328 and vimentin exchange are critical for electrophile-induced network disruption.

1. Introduction

Intermediate filaments constitute cytoskeletal structures of high plasticity that perform essential cell functions, from providing mechanical support for cell organelles, to playing critical roles in cell division, migration or response to injury or inflammation [8,12,13]. Under pathophysiological conditions, cells undergo oxidative, carbonyl or glycative stress due to the generation of increased levels of reactive species. Many of the reactive compounds, including electrophilic lipids and sugars, form covalent adducts and crosslinks in proteins altering their structure and function, and contributing to pathogenic and/or defense mechanisms [53,62]. Intermediate filaments are exquisitely sensitive to oxidative and electrophilic stress. In fact, intermediate filament proteins, including vimentin, glial fibrillary acidic protein (GFAP) and lamins are the direct targets for covalent modification by nitrosylation, lipoxidation and various types of oxidations [10,23,41,54]. Under stress conditions, intermediate filament proteins like vimentin or GFAP undergo extensive reorganization, the pattern of which displays cell-type and stimulus-dependent features [13,60]. Thus, in response to strong thiol oxidants, like diamide, fragmentation of vimentin filaments has been observed [42]. In addition, certain mediators bearing unsaturated carbonyl moieties, including

Abbreviations: 15d-PGJ_2, 15-deoxy-$\Delta^{12,14}$-prostaglandin J_2; 15d-PGJ_2-B, biotinylated 15-deoxy-$\Delta^{12,14}$-prostaglandin J_2; cyPG, cyclopentenone prostaglandin(s); DBB, dibromobimane; ECL, enhanced chemiluminiscence; EM, electron microscopy; FCCP, carbonyl cyanide 4-(trifluoromethoxy)phenylhydrazone; FRAP, fluorescence recovery after photobleaching; GFAP, glial fibrillary acidic protein; HNE, 4-hydroxynonenal; HRP, horseradish peroxidase

* Correspondence to: Department of Structural and Chemical Biology, Centro de Investigaciones Biológicas, Consejo Superior de Investigaciones Científicas (C.S.I.C.), Ramiro de Maeztu, 9, 28040 Madrid, Spain.
E-mail address: dperezsala@cib.csic.es (D. Pérez-Sala).

https://doi.org/10.1016/j.redox.2019.101098
Received 30 October 2018; Received in revised form 28 December 2018; Accepted 5 January 2019
Available online 08 January 2019

cyclopentenone prostaglandins (cyPG), induce strong bundling and/or juxtanuclear condensation of cytoplasmic intermediate filaments, which in some cases display the characteristics of aggresomes [42,60]. The biological significance of this remodeling is still not completely understood. A dual role could be hypothesized because intermediate filament remodeling could be both a mediator of cell damage and a mechanism of defense. As an amplification of damage, cells in which vimentin has undergone juxtanuclear "collapse" may display mitotic abnormalities [13]. In addition, intermediate filament proteins bearing other modifications related to oxidative stress-induced cell damage, like carbamylation, can show increased immunogenicity and behave as autoantigens in autoimmune disease [38]. On the other hand, vimentin-delimited aggresome structures could help isolating abnormally unfolded or damaged proteins for lysosomal clearance, generally through autophagy [28,34]. Moreover, intermediate filament proteins could act as decoys or scavengers of oxidants or electrophiles [1], or buffers of phosphate groups [56], serving to limit the effects of stress kinases. Indeed, nuclear lamins, which are also targets for oxidative modifications, appear to play such a role since oxidative damage is more intense in cells ectopically expressing cysteine to serine mutants of these proteins [41].

Structurally, direct modification by electrophilic species [42,54], phosphorylation [15,29,51], proteolysis [50,57], and interaction with other cytoskeletal systems [6,24,44] have been involved in vimentin remodeling induced by several agents. Phosphorylation is a main mechanism for the regulation of vimentin organization, since it can affect assembly and protein-protein interactions [15,37]. Vimentin is a substrate for a plethora of kinases, acting in physiology and pathophysiology, and phosphorylation sites are distributed all over the sequence of the protein, with special abundance in the amino-terminal end [51]. Vimentin phosphorylation has been shown to play a key role in disassembly in mitosis and in response to various stresses [32,56]. Nevertheless, the structural mechanisms underlying vimentin reorganization in response to reactive species are not completely understood. Type III intermediate filament proteins possess a conserved cysteine residue, Cys328 in vimentin, that is important for the effect of oxidants under partially denaturing conditions in vitro [47], and for vimentin reorganization in response to electrophilic compounds in cells [42]. Moreover, several mutations of this residue alter filament assembly and/or properties in cellular models [42,60]. Therefore, cysteine modification appears to be required for vimentin reorganization in response to certain stimuli. Alternatively, this cysteine residue could be involved in protein-protein interactions important for vimentin reorganization.

The vimentin intermediate filament network is a dynamic cytoplasmic structure with distinctive characteristics compared to the other cytoskeletal systems [24]. Vimentin filaments are non-polar and can grow at both ends [20]. In addition, severing and end-to-end fusion of filaments or filament fragments has been reported, both in vitro and in cells [4,35,63]. Lastly, filament subunits can be exchanged at any point along the length of the filaments [4,66]. Vimentin dynamics appears to be very active in cells, and it may involve traffic of vimentin precursors as well as exchange of subunits [42,46,66]. Subunit exchange along vimentin filaments can also take place in vitro, and rates of approximately 1% exchanged subunits per hour have been measured [35]. These special characteristics of vimentin filament organization can be important for the remodeling induced by reactive species. Here, we have addressed the morphological alterations and potential mechanisms of vimentin modification by various electrophiles in vitro and in cells. Our results indicate that lipoxidation or oxidation of vimentin before polymerization is required for filament disruption in vitro and may also be determinant in cells. Therefore, preformed filaments appear to get (lip)oxidized without undergoing significant disruption, whereas assembly or reassembly of (lip)oxidized vimentin "subunits" brings about the disruption of the network. Moreover, our results confirm the critical role of the vimentin single cysteine residue, Cys328, in network remodeling induced by electrophilic agents.

2. Materials and methods

2.1. Reagents

Electrophilic lipids 15-deoxy-$\Delta^{12,14}$-prostaglandin J_2 (15d-PGJ_2) and its biotinylated analog, and 4-hydroxynonenal (HNE), were from Cayman Chemical. Hydroxynonenal-dimethyl acetate, sodium azide, dibromobimane (DBB), dimethylsulfoxide (DMSO) and diamide were from Sigma. Carbonyl cyanide 4-(trifluoromethoxy)phenylhydrazone (FCCP) and calyculin A were from Santa Cruz Biotechnology. Anti-vimentin antibody (sc-6260) and its Alexa-488 and agarose conjugates were from Santa Cruz Biotechnology, anti-phospho-Ser56 and anti-phospho-Ser72 vimentin antibodies were from MBL, and anti-actin was from Sigma. Secondary antibodies conjugated to horseradish peroxidase (HRP) were from DAKO.

2.2. Protein preparation

Recombinant human vimentin wild type (wt) and Cys328Ser, purified essentially as described [22], were obtained from Biomedal (Spain). The protein in 8 M urea, 5 mM Tris-HCl pH 7.6, 1 mM EDTA, 10 mM 2-mercaptoethanol, 0.4 mM PMSF and approximately 0.2 M KCl (resulting from elution with a 0–0.3 M KCl gradient) was ultrafiltrated using Millipore Amicon Ultra filter units (10 K pore size) and dialyzed step-wise in 5 mM Pipes-Na pH 7.0, 1 mM DTT containing decreasing urea concentrations (8, 6 and 2 M). Final dialysis was performed for 16 h at 16 °C in 5 mM Pipes-Na, pH 7.0, 0.25 mM DTT (hypotonic buffer) [33]. The ultrafiltration step was necessary for efficient removal of metal chelators used during the purification procedure [33]. Protein concentration was estimated from its A_{280}, using an extinction coefficient of 22450 M^{-1} cm^{-1}. Aliquots of the protein were kept at − 80 °C until assayed. Throughout this work, amino acid numbering for vimentin includes the initial methionine.

2.3. Vimentin modification by oxidants and electrophiles in vitro

Modification of vimentin was assessed by gel-based techniques. Briefly, vimentin at 3.8 μM in 5 mM Pipes-Na, pH 7.0 was incubated for 60 min at room temperature in the presence of the indicated compounds. DTT final concentration was kept below 0.2 mM. Incorporation of biotinylated prostaglandins was analyzed by SDS-PAGE followed by blot and biotin detection with HRP-streptavidin. HNE adduct formation was estimated by protein immunoreactivity after SDS-PAGE and western blot with an anti-HNE adducts antibody (Calbiochem). The effect of diamide and of DMSO was assessed by electrophoresis under non-reducing conditions followed by western blot.

2.4. Electron microscopy

Vimentin polymerization was induced by incubation with 150 mM NaCl for 5 min or 1 h at 37 °C before or after treatment with electrophilic compounds. Assays were repeated at least three times and all incubation mixtures were processed in duplicate. Filaments were fixed by addition of 0.1% (v/v) glutaraldehyde. Drops of incubation mixtures were applied onto carbon support grids (MESH CF 400 CU UL, Aname), which were subsequently washed with water and stained with 2% (w/v) uranyl acetate. Grids were inspected on a JEOL transmission electron microscope JEM-1230, equipped with a digital camera CMOS TVIPS TemCam-F416. Electron microscopy (EM) images were processed with FIJI software for the measurement of filament width using the "plot profile" plugin of straightened filaments. On average, 50 filaments were measured per experimental condition.

2.5. Plasmids and transfections

The bicistronic plasmids RFP//vimentin wt and Cys328Ser, for the expression of human wt vimentin or its Cys328Ser mutant, respectively, and DSred Express2 protein (RFP) as separate products, have been previously described [42]. The backbone vector pIRES2 DSred Express2 was from Clontech. The GFP-vimentin wt fusion construct has been reported previously [54]. A synthetic sequence of the vimentin N-terminal (residues 1–136) including serine to alanine mutations on amino acids 7, 25 39, 47, 56, 65, 66, 72, 73, 83 and 87 (numbered from methionine 1), cloned in the pUC57 vector, was obtained from Genescript. This plasmid was digested with *Xho*I and the fragment subcloned into the same site of the RFP//vimentin wt vector to yield a phosphorylation-deficient ("SA") human vimentin mutant (RFP//vimentin (1–136)SA). For transient transfections, 1 μg of DNA and 3 μl of Lipofectamine 2000 (Invitrogen) were used per p35 dish, according to the manufacturer instructions.

2.6. Cell culture and treatments

SW13/cl.2 cells stably transfected with RFP//vimentin wt or RFP//vimentin Cys328Ser (RFP//vimentin wt and Cys328Ser cells, respectively) have been previously reported [42]. Cells were cultured in DMEM (Invitrogen) supplemented with 10% (v/v) fetal bovine serum (Sigma or Biowest), and antibiotics (100 U/ml penicillin plus 100 μg/ml streptomycin, Invitrogen). For maintenance of stably transfected cells, 500 μg/ml, final concentration, of G-418 (Invitrogen) were added to the culture medium. For glucose depletion, cells were washed with DMEM without glucose and cultured in this medium. For immunofluorescence, cells grown on glass coverslips were treated with vehicle (0.1% (v/v) DMSO) or electrophilic compounds in DMSO at the indicated concentrations for 2 h at 37 °C, in the absence of serum. Diamide treatment (1 mM final concentration) was carried out for 5 or 15 min, as indicated. In protection assays, cells were preincubated with DBB at 100 μM for 15 min, with 20 mM sodium azide for 15 min or 10 μM FCCP for 20 min, prior to the addition of 1 mM diamide. For calyculin A pretreatment, cells were incubated with vehicle (0.2% (v/v) DMSO) or 20 nM calyculin A in DMSO for 15 min at 37 °C before addition of diamide or 15d-PGJ_2 for 15 more min. At the end of treatments cells were washed with ice-cold PBS, fixed and processed as detailed below.

2.7. Cell lysis and western blot

For preparation of total cell lysates, cell monolayers were washed with ice-cold PBS and homogenized in 50 mM Tris-HCl pH 7.5, 0.1 mM EDTA, 0.1 mM EGTA, 0.1 mM β-mercaptoethanol, 0.5% (w/v) SDS, 20 mM sodium orthovanadate, 50 mM sodium fluoride, containing protease inhibitors (2 μg/ml each of leupeptin, aprotinin and trypsin inhibitor, and 1.3 mM Pefablock). Cell lysates were cleared of debris by centrifugation at 10,000 *g* for 5 min at 4 °C. Protein concentration was determined by the Bicinchoninic acid method (Pierce, Thermo Fisher, Rockford, IL, USA). Lysates were incubated at 95 °C for 5 min in Laemmli sample buffer and aliquots containing 30 μg of protein were analyzed by SDS-PAGE. Proteins were transferred to Immobilon-P membranes using a Semi-Dry system from Bio-Rad. Blots were blocked with 2% (w/v) non-fat dried milk and incubated with primary antibodies, typically at 1:500 dilution, and with HRP-conjugated secondary antibodies, at 1:2000 dilution, as previously described [42]. In all cases, the signal was obtained with the enhanced chemiluminiscence system (ECL) from GE Healthcare, upon exposure of the blots to Agfa Curix film.

2.8. Immunofluorescence

Cells were fixed with 4% (w/v) paraformaldehyde, permeabilized with 0.1% (v/v) Triton X-100, blocked with 1% (w/v) BSA in PBS and incubated with anti-vimentin-Alexa 488 at 1:200 dilution. After washing, cells were incubated with Phalloidin-Alexa568 (Molecular Probes) for filamentous actin (f-actin) staining. All the procedure was carried out at room temperature. Coverslips were mounted on glass slides with Fluorsave (Calbiochem). Images shown were acquired on Leica SP2, SP5 or AF6000 LX microscopes. Image analysis was performed with software from Leica (LasX) or FIJI. Particle counting was carried out with Diatrack software [59].

2.9. FRAP assays

For FRAP assays, SW13/cl.2 cells cultured on p35 glass bottom dishes (Mattek Corp.) were transiently transfected with RFP//vimentin wt (0.8 μg) plus GFP-vimentin wt (0.2 μg), and 3 μl of Lipofectamine 2000 (Invitrogen), following manufacturer instructions. Forty eight hours after transfection, cells were placed on a thermostatized chamber for observation with a Leica SP5 microscope, essentially as described previously [42]. Briefly, a prebleach image was taken, after which an area of 18 × 1.5 μm was bleached by three pulses of 488 nm laser power. Postbleach single section images were acquired every 3 s for 5 min. Fluorescence recovery was registered and plotted in recovery graphs. A minimum of twenty FRAP assays were carried out per experimental condition.

2.10. Vimentin solubility assays

RFP//vimentin wt cells were treated with the indicated agents. At the end of the treatment, cells were lysed in 20 mM Tris-HCl pH 7.4, 600 mM NaCl, 0.5% (v/v) Triton X-100, 0.1 mM sodium orthovanadate and protease inhibitors (2 μg/ml each of leupeptin, aprotinin and trypsin inhibitor, and 1.3 mM Pefablock). Lysates were centrifuged at 12,000 *g* for 10 min at 4 °C. Aliquots from pellet (30 μl, insoluble vimentin) and supernatant (15 μl, soluble vimentin) fractions were separated by SDS-PAGE and vimentin content was assessed by western blot [5,42].

2.11. ATP measurements

The luminescent ATP detection assay (Abcam) was used to measure steady-state ATP concentrations. RFP//vimentin wt cells were seeded onto 96 well glass bottom plates (1.5×10^4 cells/well) and grown for 48 h. Cells were treated with inhibitors of oxidative phosphorylation (20 mM NaN_3 for 15 min or 10 μM FCCP for 20 min), in the absence of glucose. ATP concentrations were determined in triplicate by luminescence measurement using a Varioskan Flash microplate reader (Thermo) according to the manufacturer's instructions.

2.12. Statistical analysis

All experiments were performed at least three times. Results are presented as average values ± standard error of mean (SEM). Statistical analyses were carried out using GraphPad Prism 5. For comparisons of different sets of values the Student's *t*-test was used. Differences were considered significant for $p < 0.05$. For comparison of multiple data sets the one-way analysis of variance followed by Tukey's post-test was used. Statistically significant differences are indicated on the graphs and/or in the figure legends.

3. Results

3.1. Several electrophilic species interact covalently with vimentin

In order to assess the impact of lipid electrophiles and oxidants on vimentin structure and function, we first monitored their interaction with the purified protein by means of gel-based assays. The electrophilic compound diamide is a widely used oxidant because it reacts

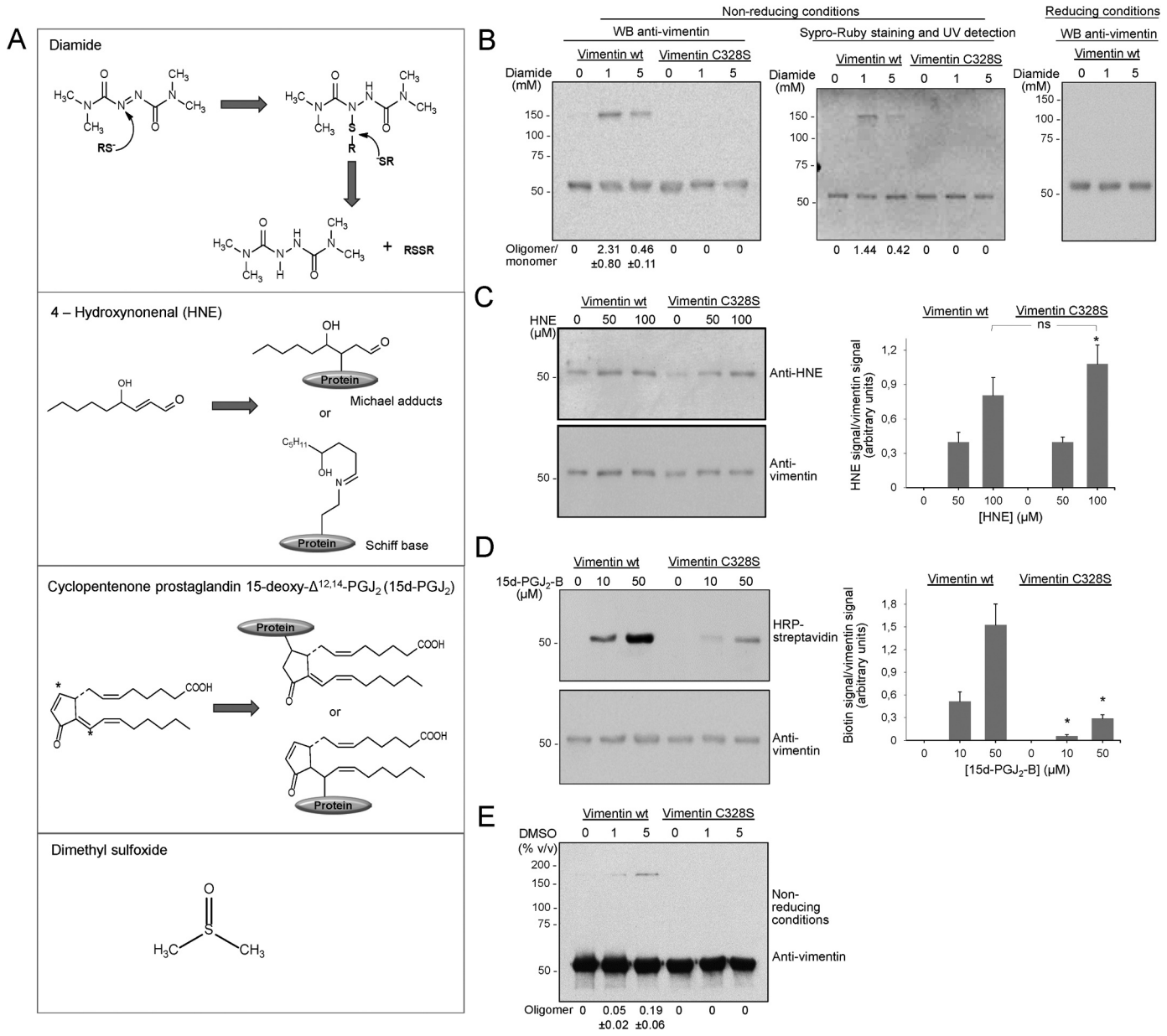

Fig. 1. Electrophilic lipids and oxidants induce covalent modification of vimentin. (A) Structures of the electrophilic lipids/compounds used and their mechanisms of adduct formation with proteins. Diamide reacts through its diazenecarbonyl moiety with thiol groups of proteins, a two-step reaction between the thiolate anion and the diazene double bond yielding a disulfide and a hydrazine [26]. 4-Hydroxynonenal (HNE) forms two types of adducts with proteins: via Schiff's base formation by reaction of the aldehydic group with an amino group of the protein and by a Michael addition to a nucleophile by the active alkene bond. The cyclopentenone prostaglandin 15-deoxy-$\Delta^{12,14}$-PGJ_2 (15d-PGJ_2) modifies proteins by Michael addition reaction through its electrophilic carbon atoms indicated with asterisks. The structure of DMSO is shown. (B) Diamide induces disulfide-bonded vimentin oligomers. Purified vimentin wild type (wt) or Cys328Ser (C328S), as indicated, was incubated at 3.8 μM in the presence of 1 or 5 mM diamide for 1 h at room temperature, after which, incubation mixtures were subjected to SDS-PAGE under reducing or non-reducing conditions and vimentin oligomeric species were visualized by western blot or total protein staining with Sypro Ruby, as indicated. The proportion of oligomer vs monomer was estimated by image scanning. (C) Modification of vimentin by HNE. Purified vimentin wt or Cys328Ser was incubated with vehicle (DMSO, 5% v/v) or HNE at 50 μM or 100 μM for 1 h. HNE adduction and vimentin levels were assessed by western blot with an anti-HNE adducts and vimentin antibodies, respectively. The signal from the anti-HNE antibody, after subtracting the background value (vehicle) was corrected by the vimentin level. (D) Modification of vimentin by biotinylated 15d-PGJ_2. Vimentin wt or Cys328Ser was incubated in the presence of vehicle (DMSO, 5% v/v) or the biotinylated analog of 15d-PGJ_2 (15d-PGJ_2-B) at 10 μM or 50 μM for 1 h. Incubation mixtures were subjected to SDS-PAGE, electrotransferred, and the incorporation of 15d-PGJ_2-B was assessed by detection of the biotin signal on blots with HRP-conjugated streptavidin. Vimentin levels were monitored by western blot. (E) Vimentin wt or Cys328Ser was incubated in the presence of the indicated concentrations of DMSO (v/v) for 1 h and the generation of disulfide-bonded oligomeric species was assessed by SDS-PAGE under non-reducing conditions and western blot and the levels of dimer were estimated in overexposed films by image scanning. The size of the molecular weight standards used (in kDa) is shown at the left of the blots. All experiments were performed at least three times and average values of the determinations ± SEM are presented either in the graphs or below the blots, except for protein staining for which a representative experiment is shown. (*$p < 0.05$ vs 50 μM HNE in panel C or vs the same condition for vimentin wt in panel D). WB, western blot.

with thiolate anions forming adducts with cysteine residues, ultimately provoking disulfide bond formation (Fig. 1A) [26]. Incubation of vimentin wt with diamide led to the formation of a vimentin oligomer, of approximately 150 kDa, which accounted for over 50% of the protein present in the incubation, and was not observed in the case of the vimentin Cys328Ser mutant (Fig. 1B). The same results were obtained by western blot with anti-vimentin antibodies and by total protein staining with Sypro-Ruby, which illustrates the purity of the protein preparation as well as the absence of other oligomeric bands. The 150 kDa oligomer is compatible with a previously characterized oxidative vimentin dimer [47], which shows an unexpectedly high electrophoretical mobility due to the elevated proportion of α-helix in this protein. This dimer appears also after cysteine crosslinking of vimentin or the related protein GFAP [42,43,47]. The dimer was not detectable when samples were analyzed under reducing conditions, indicating that is formed by disulfide bonding of vimentin (Fig. 1B).

Incubation of vimentin with HNE resulted in the formation of HNE-protein adducts, as detected by western blot with an anti-HNE adducts antibody [58]. The levels of adducts detected under these conditions were not diminished in the vimentin Cys328Ser mutant, consistent with the ability of HNE to form adducts with several nucleophilic residues (cysteine, histidine or lysine) [11] (Fig. 1C). The biotinylated analog of the cyPG 15d-PGJ_2 (15d-PGJ_2-B) formed adducts with vimentin, as previously shown by us [42]. Vimentin wt incorporated 15d-PGJ_2-B in a concentration-dependent manner, as detected by SDS-PAGE and blotting for biotin detection (Fig. 1D). In contrast, adduct formation with vimentin Cys328Ser was markedly diminished. This is consistent with the reactivity of 15d-PGJ_2, which preferentially forms adducts with cysteine residues, although one histidine adduct has been identified for Δ^{12}-PGJ_2, a cyPG with related structure [64]. Of note, lipid electrophiles used in these assays were dissolved in DMSO as vehicle. Since DMSO has been reported to oxidize cysteine [39], we also explored the putative effects of DMSO on the formation of a vimentin dimer. As shown in Fig. 1E, vimentin incubated in the presence of DMSO shows a small amount of disulfide crosslinked dimer, only detectable in over-exposed blots of non-reducing gels, which does not occur in the Cys328Ser mutant. Taken together these results show that vimentin cysteine is susceptible to modification by structurally diverse compounds, which may form adducts or induce disulfide-bonded dimers.

3.2. Effect of several oxidants and electrophiles on vimentin filament assembly in vitro

To explore the effect of reactive species on vimentin function we first used EM to assess NaCl-induced filament formation after pre-incubation with vehicle or the various agents. At early polymerization times, 5 min after addition of 150 mM NaCl, both vimentin wt and Cys328Ser formed filaments of nearly normal appearance, the ends of which could be frequently observed in the EM fields, suggesting that they had not reached their full length (Fig. 2A). Strikingly, filament formation was severely impaired in diamide pre-treated vimentin wt, which only formed polymorphic aggregates. Interestingly, when exploring the effect of lipid electrophiles, we observed that just pre-incubation in the presence of vehicle (DMSO 5% v/v) altered vimentin wt filament morphology, since filaments formed were shorter than the control, showing a 25% reduction in average length (quantitated in Fig. 2A, right panel). Preincubation with HNE resulted in filaments of an even shorter average length, accounting for a further 27% shortening with respect to the DMSO vehicle. Therefore, these observations suggest that electrophilic agents alter filament elongation or end-to-end annealing at early times of polymerization. Importantly, these alterations were absent or attenuated in vimentin Cys328Ser preincubated with either agent. Filaments formed by vimentin Cys328Ser pre-incubated in buffer (control) were longer than those of wt under the same conditions. Notably, polymerization after preincubation with diamide was totally preserved in the mutant protein. Preincubation with DMSO resulted in a non-significant 6% reduction in the average length of vimentin Cys328Ser filaments, whereas preincubation with HNE reduced average filament length by 19% with respect to DMSO. Thus, while filament shortening by DMSO was virtually abolished in the mutant vimentin, HNE still decreased the length of vimentin Cys328Ser filaments at early time points. Nevertheless, the effect of HNE was significantly attenuated in vimentin Cys328Ser with respect to the wt.

Next, we explored filament morphology at the end-point of polymerization. Vimentin wt preincubated in hypotonic buffer and then incubated with 150 mM NaCl for 1 h, formed long filaments, typically spanning several microns, showing the characteristic degree of polymorphism and an average diameter of 13.5 ± 0.3 nm (Fig. 2B), measured as exemplified in Fig. 2B, right panel. Vimentin Cys328Ser formed nearly normal filaments of 12.6 ± 0.3 nm in diameter, although at some points they showed a rougher appearance than wt. Quantitation of apparent filament diameter is shown in Fig. 2D. Diamide-preincubated vimentin wt showed even larger aggregates at this time point, connected to some filamentous structures (Fig. 2B). Interestingly, formation of filaments by diamide-treated vimentin Cys328Ser was preserved. After 1 h polymerization, filaments formed by vimentin wt preincubated with DMSO (5% v/v) reached normal length. Nevertheless they showed a consistently wider diameter (15.0 ± 0.2 nm) (Fig. 2B and D), whereas the diameter of vimentin Cys328Ser filaments was not affected by DMSO. Remarkably, HNE-induced disruption of vimentin wt was still obvious after 1 h polymerization, with formation of short filaments, frequently spanning less than one micron, for which both ends were visible in the same field at the magnification used, and displaying intense bundling. Filament width showed a marked increase, reaching a diameter of 16.9 ± 0.9 nm. Most of the HNE-induced alterations were clearly attenuated in the vimentin Cys328Ser mutant (Fig. 2B, lower panels), which showed long, individual filaments. Nevertheless, HNE pretreatment still induced a significant increase in vimentin Cys328Ser filament width with respect to preincubation with DMSO alone, although filament diameter did not reach 14 nm. Thus, in general, the morphology of vimentin Cys328Ser filaments at end point polymerization was also protected against disruption induced by pretreatment with lipoxidants with respect to the wt.

Finally, we explored the effects of the cyclopentenone 15d-PGJ_2 on filament end-point morphology (Fig. 2C). Preincubation with low concentrations of 15d-PGJ_2 did not induce major alterations, and increases in filament width were not significant with respect to the DMSO vehicle. However, with increasing concentrations (> 25 μM), filaments became more irregular and with more frequent aggregates. Vimentin Cys328Ser typically showed more entangled filaments and structures resembling knots, although individual filaments were more preserved and homogeneous than those of the wt. Nevertheless, at the highest concentrations of 15d-PGJ_2 assayed, both vimentin wt and Cys328Ser showed amorphous protein assemblies that failed to elongate.

Taken together, these results show that preincubation with oxidants or electrophiles severely impairs NaCl-induced vimentin filament formation in a manner dependent on the presence of Cys328, therefore confirming the importance of this residue in filament organization. Moreover, the morphological alterations induced show distinct features depending on the electrophilic agent.

3.3. Preformed vimentin filaments display increased resistance to disruption by lipoxidation or oxidative crosslinking

In cells, vimentin exists both in polymerized and non-polymerized forms. Therefore, we explored the susceptibility of polymerized vimentin wt to (lip)oxidation in vitro (Fig. 3). When polymerization was induced without previous incubation at room temperature, control filaments showed an average diameter of 12.3 nm, thus significantly narrower than when polymerization was started after preincubation in buffer (Fig. 3A). Interestingly, we observed that treatment of preformed vimentin filaments with diamide had little effect on filament

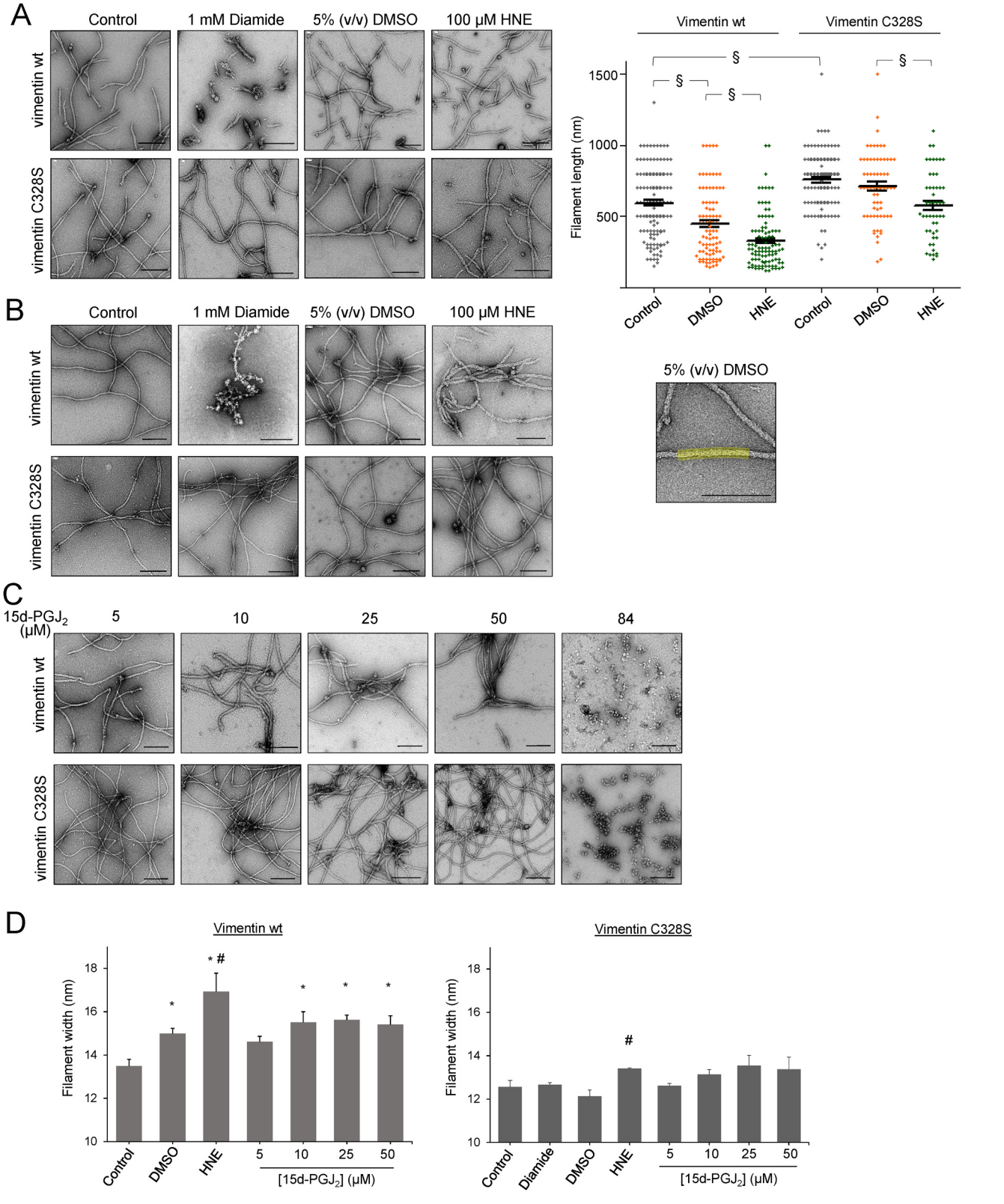

(caption on next page)

morphology, compared with the severe impairment of filament formation provoked by treatment with diamide prior to polymerization (Fig. 3A). Although DMSO still induced an increase in the width of preformed filaments, remarkably, the bundling and elongation impairment induced by both HNE and 15d-PGJ_2, and the wider diameter detected upon HNE treatment, were clearly attenuated in preformed vimentin filaments (Fig. 3A). To clarify whether the protective effect of polymerization was associated with a hindrance of chemical modification we performed gel-based assays as in Fig. 1. Curiously, polymerized vimentin underwent diamide-induced disulfide crosslinking to a similar extent than non-polymerized vimentin (Fig. 3B). Analogously, a small amount of vimentin oligomer was observed in overexposed gels

Fig. 2. Electrophilic agents and lipoxidation disrupt vimentin filament assembly in vitro. Purified vimentin wt or Cys328Ser (C328S) was preincubated with 1 mM Diamide, 5% (v/v) DMSO or 100 μM HNE for 60 min (A) and (B), or with increasing concentrations of 15d-PGJ_2 (C), after which, polymerization was induced by addition of 150 mM NaCl (final concentration), for 5 min (A) or 60 min (B) and (C). Aliquots of the incubation mixtures were processed as detailed in the Experimental Section and filaments were visualized by electron microscopy. Images shown are representative of at least three independent assays with similar results. In (A), the length of at least 50 filaments per experimental condition, except for diamide, which induced irregular aggregates, was measured, and the results are depicted in the scattered plot shown in the right panel. A p value < 0.001 was obtained for comparison between all experimental conditions by one-way analysis of variance followed by Tukey's post-test, except for vimentin Cys328Ser control vs DMSO, and vimentin wt control vs vimentin Cys328Ser HNE (non significant). In the figure, only the differences between some of the conditions are marked for clarity (§p < 0.001). In (B), the right image depicts the method for estimating filament width along segments of at least 100 nm. The graphs shown in (D) summarize width measurements under several of the experimental conditions shown in (B) and (C). Results shown are average values from at least 60 individual filaments per experimental condition ± SEM (*p < 0.05 vs control and # p < 0.05 vs DMSO by unpaired Student's *t*-test). Scale bars are 200 nm for (A)–(C) and 100 nm for (B), right panel.

upon preincubation under these conditions (2 h incubation), either in the absence or presence of DMSO. Importantly, covalent modification by HNE or 15d-PGJ_2-B was not diminished by prior polymerization, and a tendency to increase was observed at the higher concentrations. Therefore, the protective effect of previous polymerization against filament disruption does not seem to correlate with a lower modification extent. Nevertheless, the topology of the modification in the filaments could be different than in the non-polymerized protein, affecting accessible residues with little consequence on filament stability. Thus, vimentin lipoxidation or diamide-induced oxidation in vitro is more deleterious if occurring prior to assembly. Since cells possess both polymerized and non-polymerized vimentin, we set out to explore these effects in cells.

3.4. Impact of (lip)oxidation on vimentin organization in cells

The consequences of electrophile treatment were studied in vimentin-deficient SW13/cl.2 adrenal carcinoma cells, stably transfected

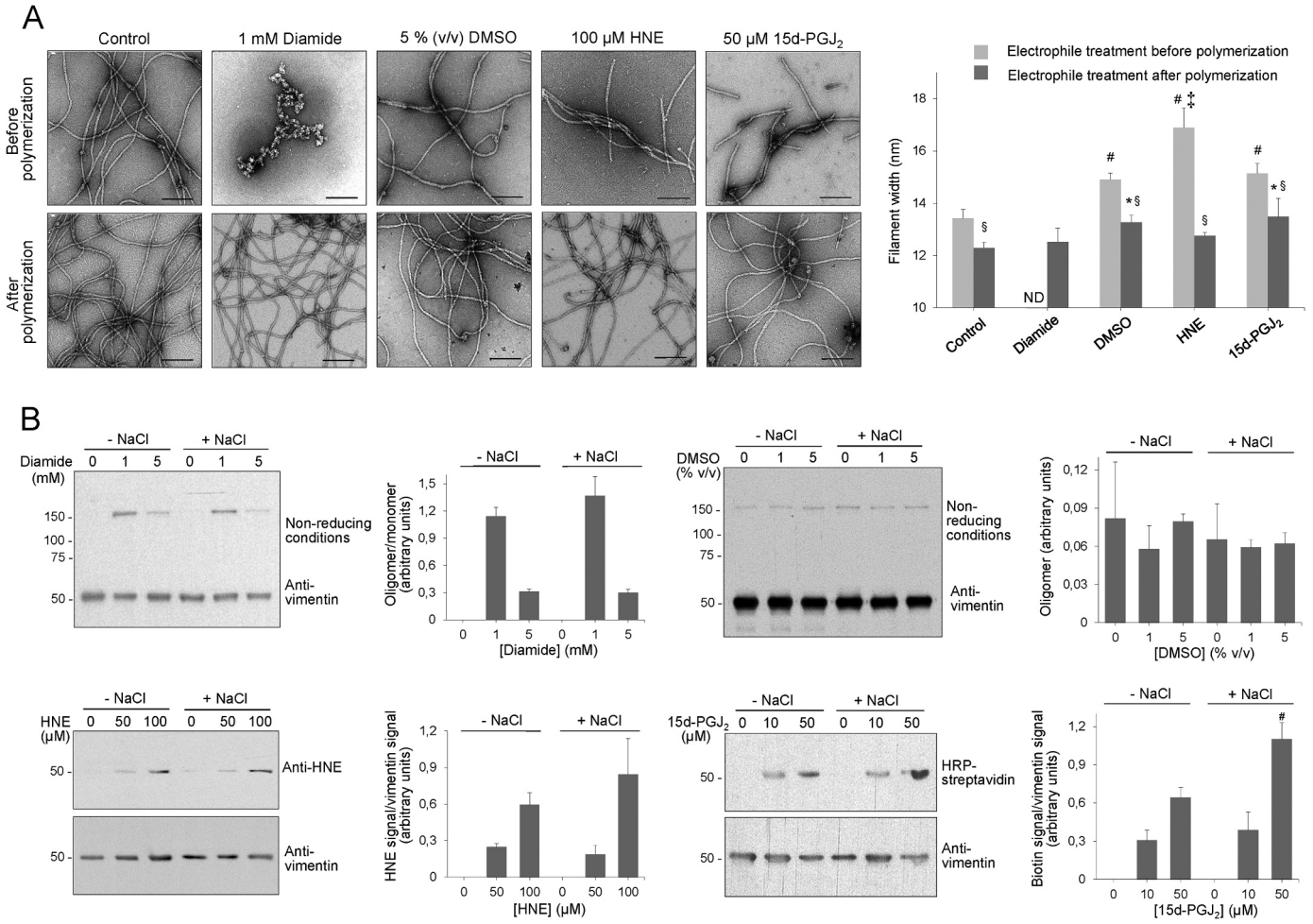

Fig. 3. Effect of oxidation or lipoxidation on the morphology of preformed vimentin filaments. Purified vimentin wt was treated in the absence (control) or presence of the indicated oxidants or electrophilic lipids before or after NaCl-induced polymerization. (A) Filament morphology was monitored by electron microscopy. Scale bars, 200 nm. The histogram in the right panel shows filament width quantitated as in Fig. 2. Results shown are average values ± SEM of 3–5 experiments totaling from 20 to 60 filaments per experimental condition. (#p < 0.05 vs control of electrophile treatment before polymerization; ‡p < 0.05 vs DMSO before polymerization; *p < 0.05 vs control of electrophile treatment after polymerization; §p < 0.05 vs the same treatment before polymerization by unpaired Student's *t*-test). ND, not determined. (B) Vimentin was incubated for 1 h at r.t. in the absence (-NaCl) or presence of NaCl (+ NaCl), after which, it was treated with the indicated oxidants or electrophilic lipids for an additional hour and the extent of modification was assessed as in Fig. 1. Results shown in graphs are average values ± SEM of three independent determinations. Comparisons were made vs the same conditions in the absence of NaCl. (# p < 0.05 vs -NaCl by paired Student's *t*-test).

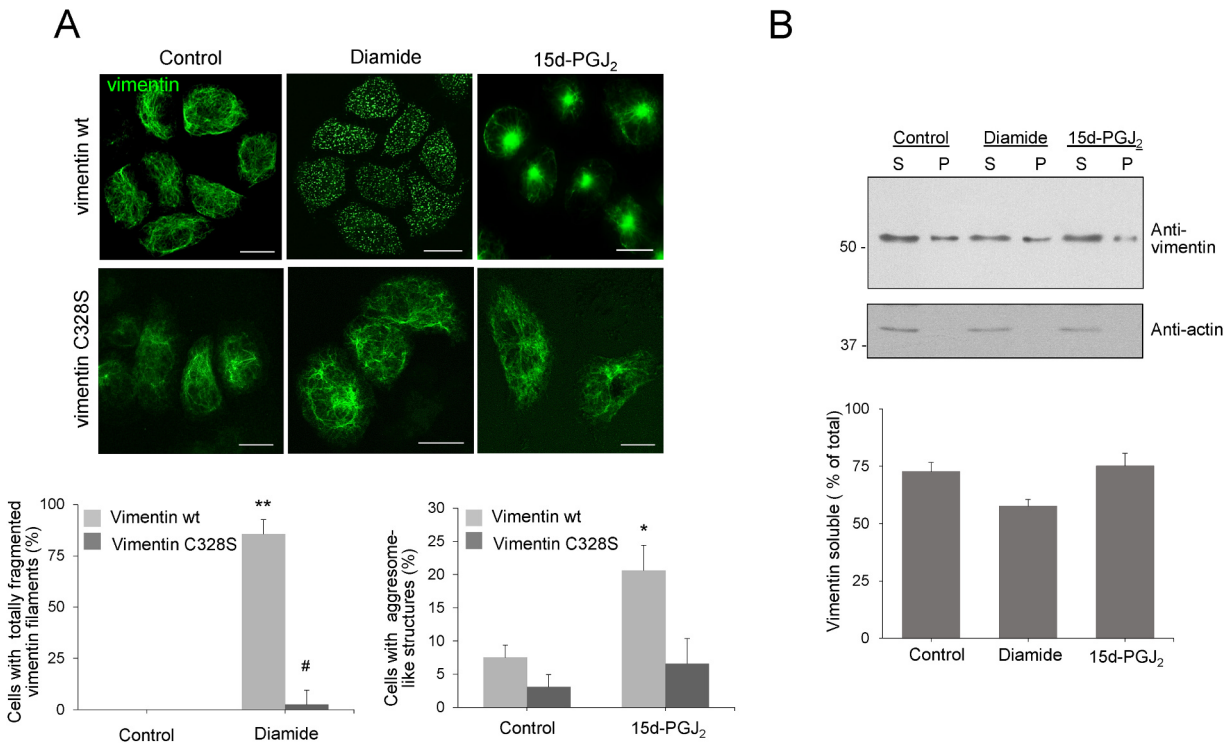

Fig. 4. Effect of electrophilic agents on vimentin organization in cells. (A) SW13/cl.2 cells stably transfected with RFP//vimentin wt or Cys328Ser (C328S) were treated with 1 mM diamide for 15 min or 10 μM 15d-PGJ_2 for 2 h, after which, cells were fixed and the vimentin network was visualized by immunofluorescence. Scale bars, 20 μm. The graphs below depict the proportion of cells with totally fragmented vimentin filaments in control or diamide treated cells (left panel), or cells with aggresome-like structures upon treatment in the absence or presence of 15d-PGJ_2 (right panel). Results are average values ± SEM of three experiments totaling at least 150 cells (**$p < 0.01$ vs control wt; #$p < 0.05$ vs diamide wt; *$p < 0.05$ vs control wt by Student's *t*-test). (B) The amount of soluble vimentin wt upon treatment with the indicated agents was monitored by cell fractionation and western blot with anti-vimentin antibody in soluble (S) and pellet (P) fractions. As a control, blots were probed with anti-actin antibody. The proportion of soluble vimentin wt was estimated by image scanning and average values obtained from three experiments ± SEM are shown in the graph.

with vimentin wt or Cys328Ser [42]. Consistent with our previous results, and shown here for reference (Fig. 4A), electrophilic agents disrupted the vimentin filament network leading to different patterns [1,42]. Diamide induced a drastic and rapid disruption of vimentin filaments leading to disperse dots, whereas 15d-PGJ_2 produced vimentin filament condensation and juxtanuclear concentration in "aggresome-like" structures (Fig. 4A). The vimentin Cys328Ser mutant showed attenuated responses to these agents, as quantitated in Fig. 4A, lower panels, being virtually resistant to the effect of diamide. This is consistent with the lack of modification of this mutant by the cyPG PGA_1-B [17] or by bifunctional cysteine crosslinkers [42] in cells. To further characterize vimentin reorganization we explored the proportion of soluble vs polymerized vimentin wt, following a high-salt/Triton X-100-based protocol according to [5]. Interestingly, these treatments did not increase the proportion of soluble vimentin wt (Fig. 4B). In fact, diamide slightly reduced soluble vimentin, an observation compatible with increased vimentin aggregation or cysteine crosslinking. Importantly, no low molecular weight vimentin fragments, indicative of degradation, were observed. Under all conditions, actin, which was used as a control of the specificity of the effects, was predominantly soluble. Therefore, vimentin reorganization by these agents does not appear to be related to increased vimentin disassembly into more soluble subunits or degradation products.

3.5. Modulation of vimentin dynamics in SW13/cl.2 cells

If, as suggested by the results obtained in vitro, preformed filaments are more resistant to disruption, cellular network fragmentation in response to diamide would require active vimentin exchange on filaments, in order that, hypothetically, reassembly of modified vimentin within the time-frame of the experiment would result in abnormal filaments. Therefore, we first assessed vimentin filament dynamics by FRAP, using cells transiently transfected with a combination of untagged vimentin wt (80%) and GFP-vimentin wt (20%) in order to highlight the vimentin filaments and perform photobleaching [42]. Reappearance of fluorescence in the targeted region could be detected few seconds after photobleaching, although total recovery required several minutes (Fig. 5A), indicating very active vimentin dynamics in this model. Nevertheless, the nature or the oligomerization state of the fluorescent vimentin incorporated into the bleached filaments cannot be ascertained with this technique. Thus, we next explored several strategies aimed at hampering vimentin dynamics. First, we employed cysteine crosslinking to "fix" vimentin filaments. The bifunctional cysteine reagent dibromobimane (DBB) irreversibly crosslinks vicinal cysteine groups within a distance of 3–6 Å [36], and selectively stabilizes the vimentin network [42]. DBB significantly prevented fluorescence recovery, indicating that it blocks vimentin exchange on filaments. Quantitative analysis of these results is shown in Fig. 5A, lower panel.

Several elegant works have shown that the exchange of subunits on vimentin filament precursors, as well as their microtubule-dependent transport, require ATP [45,46]. A commonly used strategy to lower ATP levels involves the use of inhibitors of oxidative phosphorylation, to block mitochondrial ATP synthesis, in combination with glucose depletion to limit ATP production through glycolysis [40,66]. Therefore, we incubated SW13 cells, transiently transfected with the combination of vimentin and GFP-vimentin described above, in glucose-free medium together with FCCP. This agent is an ionophore and mitochondrial oxidative phosphorylation uncoupler that disrupts ATP synthesis by transporting protons across the inner mitochondrial membrane,

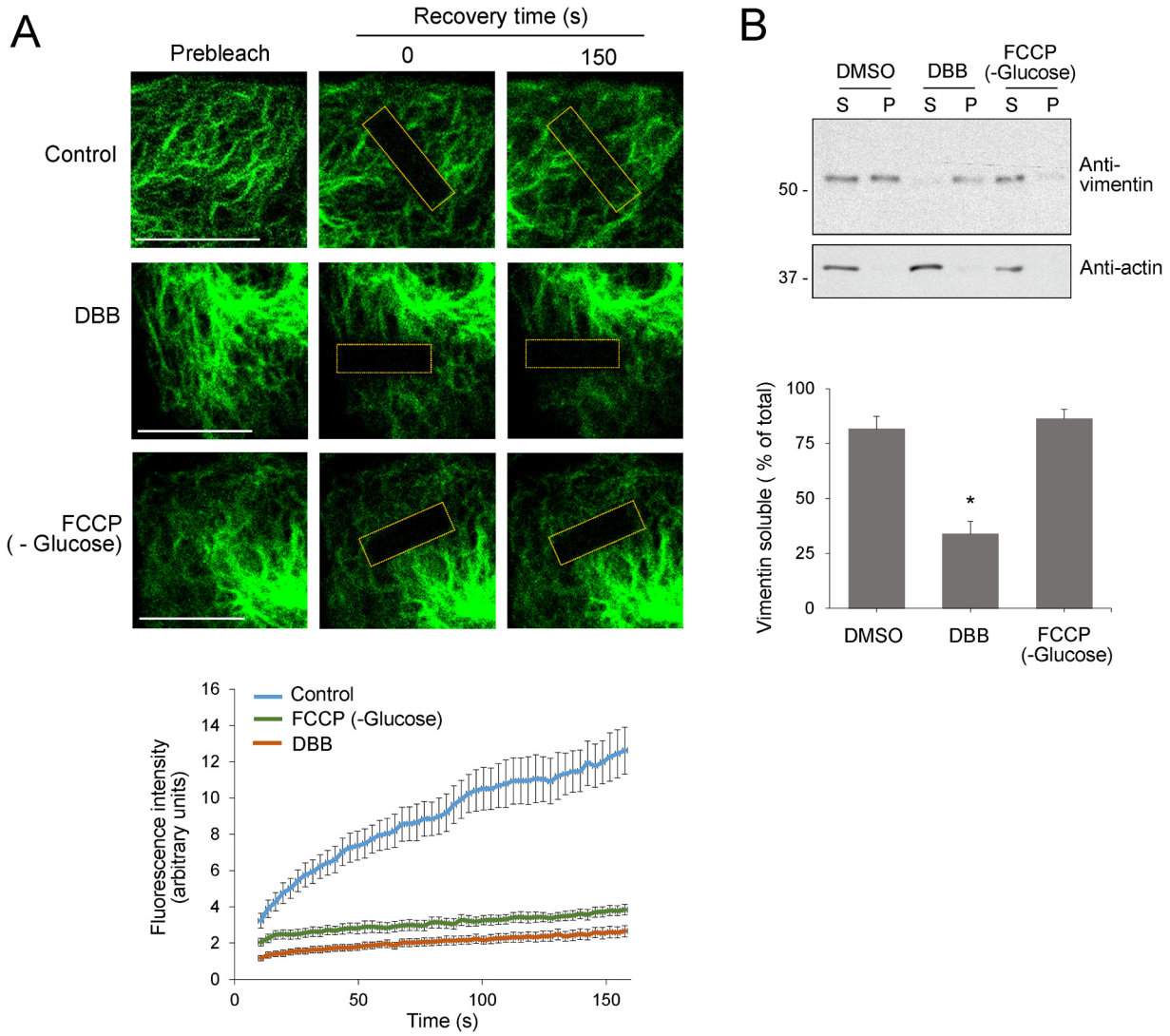

Fig. 5. Modulation of vimentin dynamics in SW13/cl.2 cells. (A) Assessment of vimentin dynamics by FRAP. SW13/cl.2 cells were transiently transfected with RFP//vimentin wt plus GFP-vimentin wt for live cell monitoring as detailed in the experimental section. FRAP assays were performed in cells treated with vehicle (control), 100 μM DBB or 10 μM FCCP in glucose-free medium for 10–30 min. Representative images acquired prior to (prebleach), immediately after (0 s) and 150 s after bleaching are shown. The bleached area is delimited by a dotted yellow rectangle. Scale bars, 10 μm. The graph shows measurements of the fluorescence intensity of the bleached area taken every 3 s. Results are average values of at least 10 determinations ± SEM. Differences between values from control and treated cells were statistically significant at all time points by Student's *t*-test. (B) Vimentin solubility under the conditions of the assays was determined as in Fig. 4. The graph depicts average values from 3 to 7 determinations ± SEM (*p < 0.05 vs DMSO (vehicle) by unpaired Student's *t*-test).

dissipating the proton gradient [3]. Recovery of fluorescence on vimentin filaments was nearly abolished in FCCP-treated, glucose-depleted cells (Fig. 5A), indicating a sharp inhibition of vimentin dynamics. Further insight into the effect of these strategies on vimentin organization was obtained from vimentin solubility assays, which showed a marked reduction in the amount of vimentin in the soluble fraction from cells treated with DBB, consistent with enhanced formation of crosslinks [42] (Fig. 5B). This effect was selective for vimentin since the amount of soluble actin was not reduced accordingly (Fig. 5B, lower blot). In contrast, FCCP plus glucose depletion apparently had no effect on vimentin solubility (Fig. 5B).

3.6. Inhibiting filament dynamics protects the vimentin network from diamide-induced disruption

To explore the impact of blocking filament dynamics on the deleterious effects of (lip)oxidation, we employed the above described strategies prior to treatment with diamide (Fig. 6). We chose diamide for these assays due to the short incubation time necessary for its effect and the clarity of the morphological changes induced: Between 80% and 90% of the cells showed total reorganization of vimentin filaments into dots after a 5 or 15 min incubation (Fig. 6A), as quantitated in Fig. 6B. Consistent with our previous observations, cysteine crosslinking with DBB completely prevented the fragmentation of vimentin filaments induced by diamide, even after a 15 min treatment [42], although a tendency of vimentin to accumulate next to the nucleus was observed. Similarly, preincubation with FCCP in glucose-free medium almost completely prevented filament fragmentation upon short-term diamide treatment (5 min). However, FCCP induced an intense condensation of vimentin filaments characteristic of aggresome formation, which has been previously reported and considered to be independent from the inhibition of oxidative phosphorylation [31]. A similar result was obtained with sodium azide, which disrupts the mitochondrial respiratory chain by inhibiting cytochrome C oxidase [55]. However, it should be noted that the protective effect of ATP-depleting approaches was attenuated after longer diamide treatments and that the use of

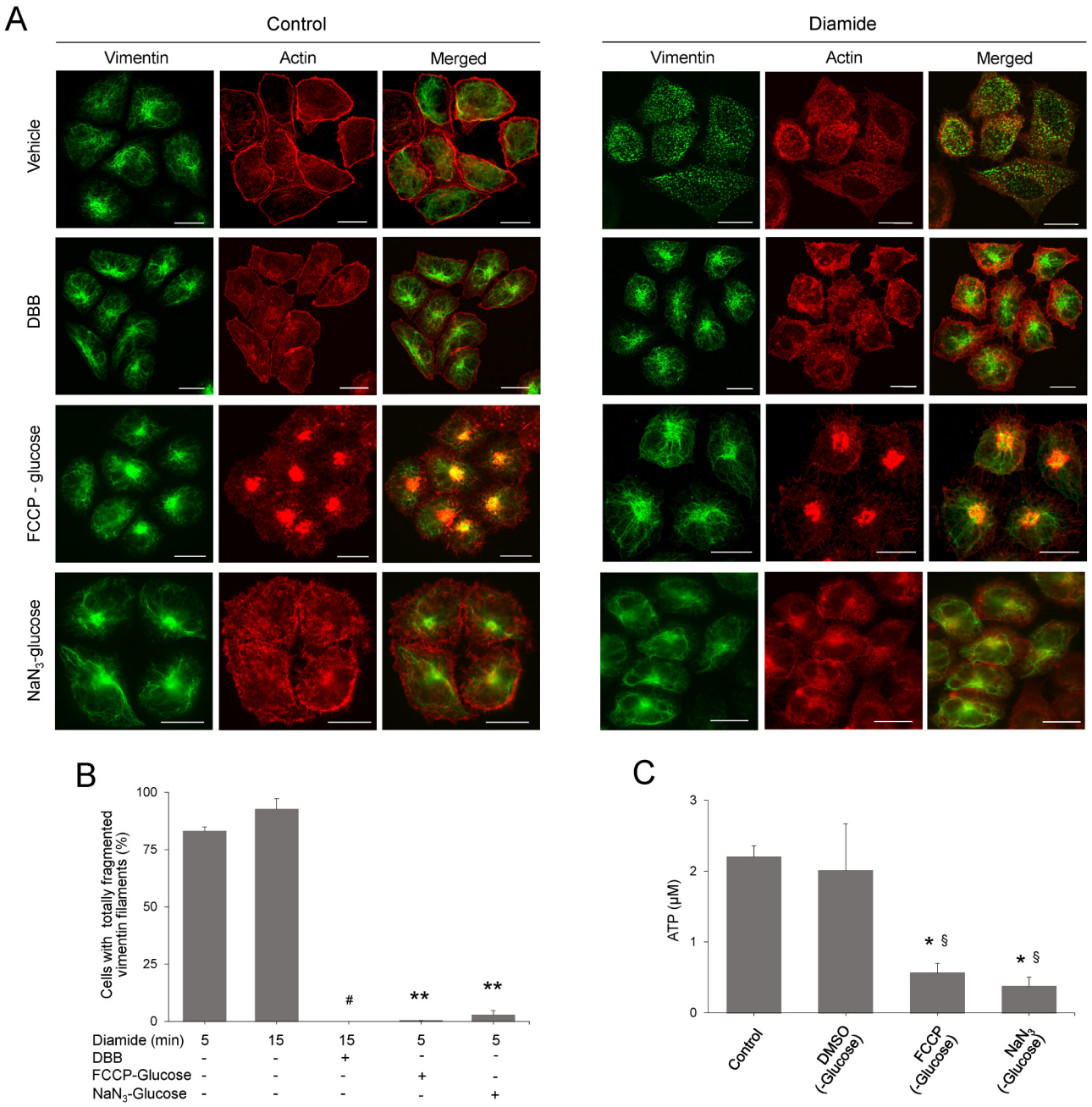

Fig. 6. Effect of inhibiting vimentin filament dynamics on diamide-induced network disruption. (A) SW13/cl.2 cells stably transfected with RFP//vimentin wt were pretreated with 100 μM DBB for 15 min in serum-free medium or with 20 mM NaN_3 or 10 μM FCCP for 15 or 20 min, respectively, in glucose- and serum-free medium, as indicated, before addition of vehicle (control, left images) or 1 mM diamide (right images) for 15 min (for DBB-pre-treated cells) or 5 min (in the case of FCCP or NaN_3-pretreated cells). Cells were fixed and vimentin distribution (green) was assessed by immunofluorescence. F-actin distribution (red) was monitored by phalloidin staining. Merged panels show the overlay of vimentin and actin signals. (B) The extent of filament severing under every condition was estimated as the proportion of cells showing completely fragmented vimentin. In every experiment, at least 300 cells were monitored per experimental condition. Results are average values ± SEM of three experiments. (**$p < 0.0001$ vs diamide 5 min, #$p < 0.05$ vs diamide 15 min). (C) Steady-state ATP levels under the different experimental conditions were determined as detailed in the experimental section. Results are presented as mean values of three experiments performed in triplicate ± SEM (*$p < 0.05$ vs control, §$p < 0.05$ vs DMSO in glucose-free medium by unpaired Student's *t*-test).

these inhibitors for longer periods or at higher concentrations was precluded by their own toxic effects. Additionally, the induction of vimentin juxtanuclear accumulation by DBB treatment or ATP depletion precluded the evaluation of the protective effects of these strategies on the perturbations of the vimentin network elicited by 15d-PGJ_2. Importantly, strategies inhibiting vimentin filament dynamics selectively protected the vimentin network vs f-actin distribution from disruption by diamide (Fig. 6A). Control cells showed a homogeneous distribution of f-actin, characterized by the presence of short cytoplasmic fibers as well as a cortical actin layer and peripheral structures typical of focal adhesions. Treatment with diamide induced f-actin disruption with appearance of a reticular pattern. Consistent with previous observations [42], pretreatment with DBB altered f-actin on its own, inducing juxtanuclear aggregation, and did not attenuate the effect of diamide. Interestingly, FCCP induced a marked alteration of f-actin per se, which predominated over the effect of diamide, characterized by a drastic accumulation coincident with the aggresome-like structure observed in some cells by vimentin immunofluorescence. Sodium azide induced a

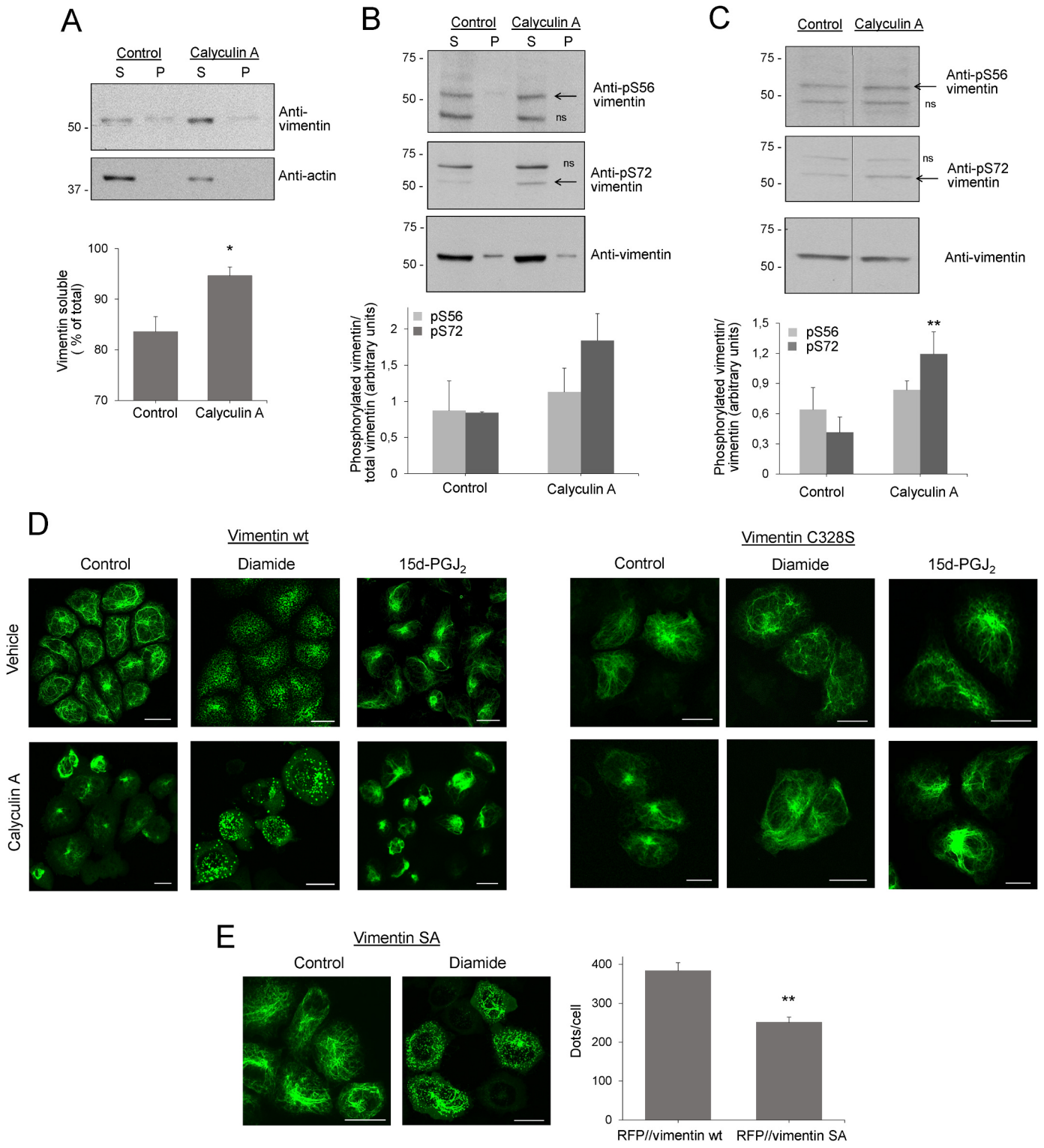

Fig. 7. Interplay between (lip)oxidation and phosphorylation in vimentin network disruption. (A) Cells stably transfected with RFP//vimentin wt were treated with vehicle (DMSO) or 20 nM calyculin A for 30 min. The effect of calyculin A on vimentin solubility was assessed as in Fig. 4. The graph depicts average results from three determinations ± SEM (*p < 0.05 vs control by paired Student's *t*-test). The levels of phospho-Ser56 (pS56) and phospho-Ser72 (pS72) vimentin were estimated by western blot with phosphospecific antibodies in soluble and pellet fractions (B) or in total cell lysates (C). The position of phosphorylated vimentin is indicated by arrows and that of non-specific bands, marked as "ns". In (C), dotted lines show where lanes from the same gel have been cropped. The graphs in (B) and (C) show the ratio of phosphorylated vimentin vs total vimentin, in soluble fractions (B) or total cell lysates (C), as average values ± SEM from three independent assays. (**p < 0.01 vs control). (D) Cells stably transfected with RFP//vimentin wt or Cys328Ser (C328S) were pretreated with vehicle (DMSO) or 20 nM calyculin A for 15 min, after which, 1 mM diamide or 50 μM 15d-PGJ_2 were added for 15 more min and cells were fixed and processed for detection of vimentin by immunofluorescence. (E) SW13/cl.2 cells were transiently transfected with the phosphorylation-deficient mutant RFP//vimentin SA and 48 h after transfection they were treated with 1 mM diamide for 15 min. The distribution of vimentin was assessed by immunofluorescence. The degree of filament fragmentation was estimated by counting the number of vimentin particles per cell using the Diatrack software. The histogram shows the number of dots per cell (mean ± SEM) obtained from 40 cells measured in three independent experiments (**p ≤ 0.0001 vs the dots per cell in diamide-treated, vimentin wt-expressing cells by unpaired Student's *t*-test).

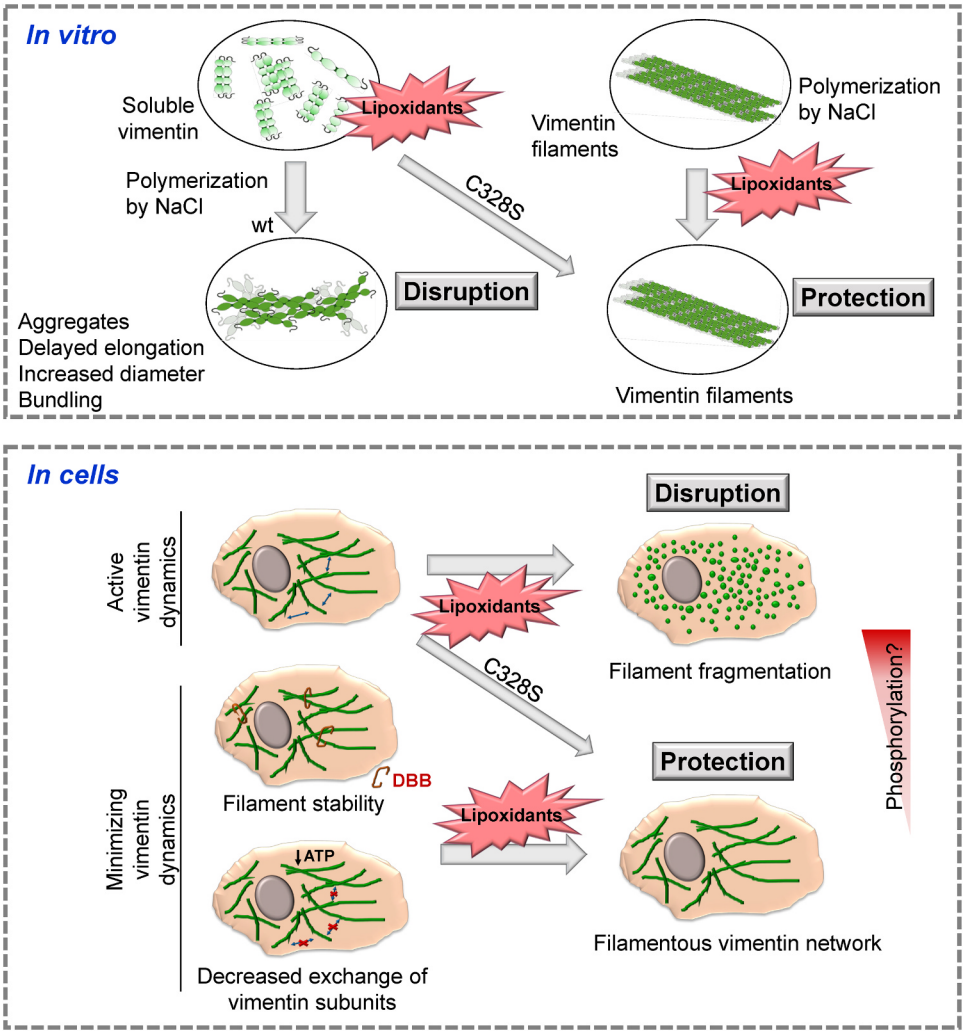

Fig. 8. Importance of vimentin dynamics for the disruption of vimentin filaments induced by (lip)oxidation. In vitro, pre-incubation of soluble vimentin with electrophilic lipids and/or oxidants (lipoxidants) hampers subsequent filament formation induced by NaCl, leading to impaired elongation and/or aggregates, filaments of increased diameter or filament bundles, in a manner dependent on the presence of Cys328. In contrast, lipoxidation of preformed filaments does not severely alter filament morphology. In cells with active vimentin dynamics, lipoxidants induced filament fragmentation or condensation of vimentin wt, but not Cys328Ser (C328S). Minimizing vimentin dynamics protects the morphology of the vimentin wt network upon (lip)oxidation. Phosphorylation may contribute to vimentin network disruption induced by electrophilic compounds. Taken together these observations suggest that incorporation of modified vimentin subunits into filaments would be the process leading to network disruption.

bristly appearance of f-actin per se, but it did not improve the disruption induced by diamide.

The efficacy of the various approaches used for cellular ATP depletion prior to treatment with diamide was confirmed by measuring total ATP levels, which showed a significant decrease of steady-state ATP levels in cells treated with FCCP or sodium azide in glucose-free medium (Fig. 6C).

3.7. Interplay between phosphorylation and (lip)oxidation in vimentin network reorganization

Vimentin hyperphosphorylation elicited by phosphatase inhibitors has been reported to induce vimentin disassembly in some experimental models [15]. Therefore, we hypothesized that, if blocking dynamics protected vimentin from (lip)oxidation-induced remodeling, inducing disassembly through phosphorylation might have the opposite effect. Treatment of RFP//vim wt cells with the phosphatase 1 and 2 A inhibitor calyculin A (20 nM for 15 min) induced an increase in the proportion of vimentin in the soluble fraction, indicating disassembly (Fig. 7A). In addition, upon calyculin A treatment, levels of phospho-Ser72 vimentin tended to increase in the soluble fraction (Fig. 7B) and significantly augmented in total cellular lysates (Fig. 7C). Longer pretreatments or higher concentrations of calyculin A could not be used due to cell toxicity. Morphologically, calyculin A induced coalescence of vimentin filaments together with the appearance of a more diffuse cellular background, although no filament fragmentation was observed (Fig. 7D, left panels). Interestingly, pretreatment with calyculin A intensified the disruption of the vimentin wt network induced by electrophilic agents (Fig. 7D, left lower images). Thus, in calyculin A-pretreated cells diamide induced intense filament fragmentation and aggregates formation, together with the appearance of diffuse cytoplasmic vimentin, suggesting that both agents cooperate in filament disruption. In turn, 15d-PGJ_2-induced network disorganization was also potentiated by calyculin-A pretreatment, resulting in amorphous condensations and loss peripheral filaments.

Importantly, vimentin Cys328Ser was resistant to disruption by either of these agents alone or in combination (Fig. 7D, right panels), and filaments were better preserved, which stresses the importance of cysteine modification for vimentin remodeling even in the presence of phosphatase inhibitors.

As an initial approach to estimate the potential contribution of vimentin phosphorylation to filament disruption by electrophilic agents, we explored the response of a phosphorylation-deficient vimentin “SA mutant”, previously used in studies with cellular and animal models [32], in which 11 phosphorylatable serine residues present in the protein N-terminus, have been substituted for alanines (Fig. 7E). The SA vimentin mutant formed full filaments, although with a more irregular appearance than those of wt. Diamide treatment induced an intense fragmentation of the vimentin SA network, although longer filament fragments coexisted with dots in some cells (Fig. 7E). Quantitation of the extent of disruption as the number of filament fragments detected per cell showed a less exhaustive filament severing of the vimentin SA network than of the vimentin wt (Fig. 7E, right panel). Nevertheless, these results should be taken cautiously, since it cannot be discarded

that the multiple substitutions may affect the structure or assembly of this mutant in a way not yet characterized.

Taken together these results indicate that phosphorylation and oxidative modifications may cooperate in the disruption or remodeling of the vimentin network in response to electrophilic agents. However, cysteine modification appears to be a strict requirement.

4. Discussion

The vimentin network is a highly dynamic structure capable of rapid rearrangements, which in the course of seconds or a few minutes can lead to extensive filament remodeling in response to oxidants, heat shock and several types of stress [19,30,54]. Vimentin is a critical sensor for oxidative or nitrosative stress [23], and is the target for lipoxidation by several electrophilic lipids [42]. Both types of modification induce marked vimentin network reorganization. Here, we have addressed the mechanisms underlying these effects. Our results show that in vitro, vimentin (lip)oxidation prior to assembly is deleterious for filament formation, resulting in morphological alterations including aggregation, increased filament diameter, heterogeneity and/or bundling. However, (lip)oxidation of preformed filaments is better tolerated. These effects have a clear counterpart in cells, where (lip)oxidation induces a marked reorganization of the vimentin network. Nevertheless, blocking vimentin dynamics effectively preserves network morphology. These observations indicate that for electrophiles to disrupt vimentin organization, active dynamics/subunit exchange should be taking place. Therefore, it could be speculated that modifications of assembled filaments do not severely disrupt the network and that the critical step in the remodeling of vimentin would be the reassembly of "(lip)oxidized subunits". These observations are summarized in the scheme shown in Fig. 8.

The in vitro experiments herein reported show the modification of vimentin by various electrophilic species, which can be detected by immunological techniques or tagged analogs of reactive lipids. Electrophile-induced modification of vimentin follows patterns related to the reactivity of the various species. Thus, diamide induces disulfide bonding, therefore dependent on the presence of the single vimentin cysteine, Cys328. In contrast, HNE, which has a broader reactivity and can form both Michael adducts with various nucleophilic residues and Schiff bases with amino groups, forms adducts with both vimentin wt and the Cys328Ser mutant. Although Cys328 has been reported as the main site of addition of HNE in vimentin in biological systems [7], our results indicate that, in vitro, other sites can be adducted by HNE when Cys328 is not present. The cyPG 15d-PGJ_2 can form Michael adducts with cysteine, although adducts of other cyPG, namely, Δ^{12}-PGJ_2, with histidine residues have been reported [64]. Under our conditions, 15d-PGJ_2-B preferentially modifies vimentin wt, confirming that Cys328 is the main target for lipoxidation by this species. This is consistent with experiments in several cell types, showing that modification and disruption of vimentin Cys328Ser by electrophilic species was attenuated with respect to the wt [17,42,54]. Cys328 has been reported to be the target for several oxidative modifications, besides lipoxidation, including thiolation, glutathionylation and nitrosylation [14,16,25]. This indicates that this cysteine residue is particularly reactive. Nevertheless, these modifications, and in particular lipoxidation, affect selected cysteine residues in other proteins including actin, tubulin, heat shock proteins or elongation factors, among others. Indeed, we have previously reported that lipoxidation by cyPG affects a selective subset of reactive proteins in cells [49], among which vimentin arises as a major target [54].

The reactive species responsible for vimentin modification can then be very varied. This means that the cysteine residue can be decorated by structurally diverse moieties. Importantly, the functional consequences of (lip)oxidation also present a structure-dependent pattern. Thus, in vitro, diamide induces irregular vimentin aggregation and a profound disruption of filament morphology. The effect of DMSO on oxidative modifications is seldom reported [39]. Nevertheless, we realized that preincubation with DMSO alone reduced filament length at early polymerization times and induced an increase in the apparent diameter of vimentin wt, but not Cys328Ser filaments at end-point polymerization. Therefore, this effect could be related, at least in part, to oxidative modifications of the cysteine residue, reflected by the appearance of the vimentin disulfide-bonded dimer in DMSO-treated vimentin wt. Treatment with HNE led to the formation of filaments that appeared even shorter and thicker at early and late time-points of polymerization, respectively. 15d-PGJ_2 induced miscellaneous alterations. Interestingly, even preincubation in buffer before polymerization results in wider filaments than when polymerization is induced without delay (13.4 nm vs 12.3 nm, Fig. 3A), thus suggesting that some oxidation occurring during preincubation affects filament assembly. This possibility is also supported by the observation that filaments formed at early polymerization times, induced after 1 h preincubation, achieve a greater length in the case of vimentin Cys328Ser than the wt (Fig. 2A). The information from the structural models available [27], together with previous evidence, could lead to at least two hypotheses to explain the observed variations in diameter: either there could be an increased separation between vimentin subunits or a higher number of subunits per filament section. Indeed, vimentin filaments are polymorphic and can comprise a variable number of tetramers per section [35]. Whereas the most accepted model comprises eight tetramers per section [2,52], up to 12 tetramers have been observed in some settings, and even 24, depending on the assembly conditions and the presence of certain divalent cations [21]. In addition, the presence of a low proportion of oxidatively modified vimentin or of disulfide-crosslinked dimers could affect the overall disposition of vimentin tetramers in the filament, affecting filament elongation as well. Further work would be necessary to ascertain these possibilities. Taken together these results suggest that filament elongation and diameter are highly sensitive to vimentin (lip) oxidative modifications.

Importantly, most morphological alterations are either blunted or attenuated in the vimentin Cys328Ser mutant, thus illustrating the functional importance of this residue for filament assembly and as a sensor for electrophilic or oxidative stress. Thus, Cys328 is emerging both as a hot spot for posttranslational modification in vimentin and as a switch or hinge influencing the assembly of the protein.

Remarkably, although in preformed filaments modification by electrophiles occurs to the same or even higher extent than in unassembled vimentin, its functional outcome is markedly attenuated. This could imply that in preformed filaments modification occurs at exposed sites that do not severely interfere with filament structure, nor induces filament unravelling or disassembly. In contrast, modification of isolated subunits appears to interfere with subsequent assembly. This could be the result of steric hindrance due to the adducted moiety. Alternatively, modification of Cys328 could induce conformational changes in isolated subunits which would not occur once integrated in filaments or, contrariwise, preclude conformational changes needed for assembly or maturation of filaments. In particular, disulfide bonds could form between cysteine residues located within close distance in assembled filaments without inducing disruption, whereas in isolated subunits they could elicit associations not suitable for further assembly or elongation.

In summary, our in vitro results can be recapitulated as follows: Mild oxidation of vimentin (as that elicited by preincubation with buffer or DMSO) associates with shorter filaments at early time points of polymerization and with an increase in filament width at end-point polymerization that are dependent on the presence of Cys328. Diamide induces a drastic perturbation of filament assembly both at early and late time points, which require Cys328 and does not take place in polymerized filaments. HNE pretreatment leads to shorter filaments than those formed after DMSO pretreatment, both at early time points and at end-point polymerization, at which time intense filament bundling and a wider diameter are also apparent. Among HNE-induced

alterations, shortening and bundling at end-point polymerization require Cys328, whereas all alterations are attenuated in preformed filaments. Pretreatment with 50 μM15d-PGJ_2 correlates with more intense bundling and irregular filament shape, both of which are attenuated in Cys328Ser vimentin, as well as in vimentin wt preformed filaments.

The oxidant diamide poses an interesting case, because it induces an intense disruption of vimentin polymerization, which is clearly dependent on the presence of Cys328. Therefore, we have used diamide as a model electrophilic compound in cells, together with the cyPG 15d-PGJ_2. Nevertheless, the nature of the modification induced by diamide is not completely understood. Although a disulfide-bonded vimentin dimer is clearly formed in vitro, it was not observed in cells [42], in which mixed disulfides with small molecules resulting in glutathionylation or cysteinylation could also occur. Alternatively, in short-term treatments, the diamide adduct (Fig. 1A) could also be present. These possibilities will be the object of future studies.

In cells, filaments are subjected to continuous exchange, although the nature of the "subunits" being exchanged (whether they are tetramers, unit-length filaments or filament fragments) and the rate at which this exchange occurs are not completely understood. Under our experimental conditions FRAP occurred within seconds/minutes, indicative of active filament dynamics, meaning "subunit" shedding and reincorporation.

When we applied treatments intended to minimize vimentin dynamics, the rate of fluorescence recovery was blunted. Under these conditions we observed nearly full protection of the vimentin network against diamide-induced disruption. This suggests that, as observed in vitro, preformed filaments may be resistant to disruption, which leads us to hypothesize that disruption occurs when (lip)oxidized vimentin "subunits" attempt to incorporate into filaments. The motile properties of vimentin filaments are known to require ATP [66]. However, the mechanism by which inhibitors of ATP synthesis block vimentin dynamics is not fully understood. From the comparison of the initial and final images of FRAP experiments it appears that ATP depletion also reduces global filament movement, although subunit exchange is considered to be independent from full filament motility [61]. Regarding subunit exchange, it has been hypothesized that ATP could be necessary for phosphorylation of vimentin or for the action of an ATP-dependent cofactor (kinase or chaperone) that would contribute to tetramer dissociation and prevent reassembly [46]. Nevertheless, the possibility that the protective effect of mitochondrial uncouplers could be due to their impact on other mitochondrial functions or to the contribution of indirect mechanisms, cannot be discarded.

Vimentin disassembly in response to various stimuli and during mitosis is related to an increase in phosphorylation. Several kinases, the target residues of which concentrate in the N-terminus of the protein, act in a concerted way during mitosis to promote disassembly in a cell type-dependent manner [9,65]. In particular, Ser39 and Ser72 are phosphorylated by AuroraB, and/or RhoK [18,32], and mutation of the target phosphorylation sites at the N-terminus of the protein leads to mitotic abnormalities. Moreover, phosphorylation by PKA in interphase, which occurs at multiple sites of the protein, leads to vimentin disassembly [15]. In addition, microinjection of the catalytic subunit of PKA has been reported to induce vimentin bundling and in extreme cases, fragmentation into dots similar to those observed here with diamide [29]. We attempted to increase the proportion of phosphorylated vimentin by incubation with the phosphatase inhibitor calyculin A. This effectively increased the level of phosphorylated vimentin and the proportion of soluble vimentin, and altered the vimentin network. When combined with (lip)oxidation agents we observed a more intense disruption. This, together with the fact that a phosphorylation-deficient vimentin mutant showed a partial but significant protection from diamide-induced fragmentation suggests that phosphorylation and (lip) oxidation can cooperate in network disruption. Indeed, in cells, oxidative stress or electrophilic agents could also lead to inhibition of phosphatases, as has been described for phosphatases 1 and 2A [48], leading to vimentin hyperphosphorylation. Nevertheless, the contribution of the phosphorylation of other proteins to the effects of phosphatase inhibitors cannot be excluded.

A critical observation is that vimentin Cys328Ser appears to be completely protected from filament fragmentation, even in the presence of calyculin A and diamide, which reinforces the role of the cysteine residue as a gatekeeper of vimentin organization, either by direct modification or by indirect mechanisms. It would be interesting to explore whether this mutant is also protected from alterations of the vimentin network induced by other stimuli.

Altogether we have demonstrated the severe impact that oxidative and electrophilic modifications can have on vimentin assembly in vitro and in cells, and proposed their interplay with phosphorylation levels in the cellular context, which could further modulate the intermediate filament network. The consequences that alterations in these regulatory connections may have in a pathophysiological context, during aging or mitosis will most probably depend on the extent of the oxidative damage and the activation/inactivation of redox-responsive kinases and phosphatases.

Acknowledgements

This work was supported by the European Union's Horizon 2020 research and innovation program under the Marie Sklodowska-Curie Grant agreement no. 675132 "Masstrplan", Grant SAF2015-68590-R from MINECO/FEDER, Spain and Instituto de Salud Carlos III/FEDER, RETIC Aradyal RD16/0006/0021. Feedback from COST Action CA15214 "EuroCellNet" is gratefully acknowledged. We wish to thank M.T. Seisdedos and G. Elvira from CIB, CSIC, for expert assistance with confocal microscopy and FRAP assays. We are indebted to F. Escolar and Drs. R. Núñez and B. Pou from CIB, CSIC, for valuable help with electron microscopy.

References

[1] G. Aldini, M.R. Domingues, C.M. Spickett, P. Domingues, A. Altomare, F.J. Sánchez-Gómez, C.L. Oeste, D. Pérez-Sala, Protein lipoxidation: detection strategies and challenges, Redox Biol. 5 (2015) 253–266.

[2] S. Ando, K. Nakao, R. Gohara, Y. Takasaki, K. Suehiro, Y. Oishi, Morphological analysis of glutaraldehyde-fixed vimentin intermediate filaments and assembly-intermediates by atomic force microscopy, Biochim. Biophys. Acta 1702 (2004) 53–65.

[3] R. Benz, S. McLaughlin, The molecular mechanism of action of the proton ionophore FCCP (carbonylcyanide p-trifluoromethoxyphenylhydrazone), Biophys. J. 41 (1983) 381–398.

[4] G. Colakoglu, A. Brown, Intermediate filaments exchange subunits along their length and elongate by end-to-end annealing, J. Cell Biol. 185 (2009) 769–777.

[5] L. Chang, K. Barlan, Y.H. Chou, B. Grin, M. Lakonishok, A.S. Serpinskaya, D.K. Shumaker, H. Herrmann, V.I. Gelfand, R.D. Goldman, The dynamic properties of intermediate filaments during organelle transport, J. Cell Sci. 122 (2009) 2914–2923.

[6] L. Chang, R.D. Goldman, Intermediate filaments mediate cytoskeletal crosstalk, Nat. Rev. Mol. Cell Biol. 5 (2004) 601–613.

[7] J. Chavez, W.G. Chung, C.L. Miranda, M. Singhal, J.F. Stevens, C.S. Maier, Site-specific protein adducts of 4-hydroxy-2(*E*)-nonenal in human THP-1 monocytic cells: protein carbonylation is diminished by ascorbic acid, Chem. Res. Toxicol. 23 (2010) 37–47.

[8] F. Cheng, J.E. Eriksson, Intermediate filaments and the regulation of cell motility during regeneration and wound healing, Cold Spring Harb. Perspect. Biol. 9 (9) (2017) a022046 (pii).

[9] Y.H. Chou, S. Khuon, H. Herrmann, R.D. Goldman, Nestin promotes the phosphorylation-dependent disassembly of vimentin intermediate filaments during mitosis, Mol. Biol. Cell 14 (2003) 1468–1478.

[10] F. Di Domenico, R. Coccia, A. Cocciolo, M.P. Murphy, G. Cenini, E. Head, D.A. Butterfield, A. Giorgi, M.E. Schinina, C. Mancuso, C. Cini, M. Perluigi, Impairment of proteostasis network in Down syndrome prior to the development of Alzheimer's disease neuropathology: redox proteomics analysis of human brain, Biochim. Biophys. Acta 1832 (2013) 1249–1259.

[11] M.R. Domingues, P. Domingues, T. Melo, D. Pérez-Sala, A. Reis, C. Spickett, Lipoxidation adducts with peptides and proteins: deleterious modifications or signalling mechanisms? J. Proteom. 92 (2013) 110–131.

[12] G. dos Santos, M.R. Rogel, M.A. Baker, J.R. Troken, D. Urich, L. Morales-Nebreda, J.A. Sennello, M.A. Kutuzov, A. Sitikov, J.M. Davis, A.P. Lam, P. Cheresh, D. Kamp, D.K. Shumaker, G.R. Budinger, K.M. Ridge, Vimentin regulates activation of the

NLRP3 inflammasome, Nat. Commun. 6 (2015) 6574.
[13] S. Duarte, Á. Viedma-Poyatos, E. Navarro, A.E. Martínez, M.A. Pajares, D. Pérez-Sala, Vimentin filaments interact with the mitotic cortex allowing normal cell division, BioRxiv (2018), https://doi.org/10.1101/356642.
[14] P. Eaton, M.E. Jones, E. McGregor, M.J. Dunn, N. Leeds, H.L. Byers, K.Y. Leung, M.A. Ward, J.R. Pratt, M.J. Sgattock, J. Am. Soc. Nephrol. 14 (2003) S290–S296.
[15] J.E. Eriksson, T. He, A.V. Trejo-Skalli, A.-S. Härmälä-Braskén, J. Hellman, Y.-H. Chou, R.D. Goldman, Specific in vivo phosphorylation sites determine the assembly dynamics of vimentin intermediate filaments, J. Cell Sci. 117 (2004) 919–932.
[16] M. Fratelli, H. Demol, M. Puype, S. Casagrande, I. Everini, M. Salmona, V. Bonetto, M. Mengozzi, F. Duffieux, E. Miclet, A. Bachi, J. Vanderkerckhove, E. Giannaza, P. Ghezzi, Identification by redox proteomics of glutathionylated proteins in oxidatively stressed human T lymphocytes, Proc. Natl. Acad. Sci. USA 99 (2002) 3505–3510.
[17] S. Gharbi, B. Garzón, J. Gayarre, J. Timms, D. Pérez-Sala, Study of protein targets for covalent modification by the antitumoral and anti-inflammatory prostaglandin PGA_1: focus on vimentin, J. Mass Spectrom. 42 (2007) 1474–1484.
[18] H. Goto, H. Kosako, K. Tanabe, M. Yanagida, M. Sakurai, M. Amano, K. Kaibuchi, M. Inagaki, Phosphorylation of vimentin by Rho-associated kinase at a unique amino-terminal site that is specifically phosphorylated during cytokinesis, J. Biol. Chem. 273 (1998) 11728–11736.
[19] B.P. Helmke, R.D. Goldman, P.F. Davies, Rapid displacement of vimentin intermediate filaments in living endothelial cells exposed to flow, Circ. Res. 86 (2000) 745–752.
[20] H. Herrmann, U. Aebi, Intermediate filaments: molecular structure, assembly mechanism, and integration into functionally distinct intracellular scaffolds, Annu. Rev. Biochem. 73 (2004) 749–789.
[21] H. Herrmann, M. Haner, M. Brettel, N.O. Ku, U. Aebi, Characterization of distinct early assembly units of different intermediate filament proteins, J. Mol. Biol. 286 (1999) 1403–1420.
[22] H. Herrmann, I. Hofmann, W.W. Franke, Identification of a nonapeptide motif in the vimentin head domain involved in intermediate filament assembly, J. Mol. Biol. 223 (1992) 637–650.
[23] B. Huang, S.C. Chen, D.L. Wang, Shear flow increases S-nitrosylation of proteins in endothelial cells, Cardiovasc. Res. 83 (2009) 536–546.
[24] F. Huber, A. Boire, M.P. Lopez, G.H. Koenderink, Cytoskeletal crosstalk: when three different personalities team up, Curr. Opin. Cell Biol. 32 (2015) 39–47.
[25] J. Jia, A. Arif, F. Terenzi, B. Willard, E.F. Plow, S.L. Hazen, Target-selective protein S-nitrosylation by sequence motif recognition, Cell 159 (2014) 623–634.
[26] P. Fox, N.S.L. Kosower, E.M. Kosower, Formation of disulfides with diamide, Methods Enzymol. 143 (1987) 264–270.
[27] L. Kreplak, U. Aebi, H. Herrmann, Molecular mechanisms underlying the assembly of intermediate filaments, Exp. Cell Res. 301 (2004) 77–83.
[28] T. Lamark, T. Johansen, Aggrephagy: selective disposal of protein aggregates by macroautophagy, Int. J. Cell Biol. 2012 (2012) 736905.
[29] N.J. Lamb, A. Fernandez, J.R. Feramisco, W.J. Welch, Modulation of vimentin containing intermediate filament distribution and phosphorylation in living fibroblasts by the cAMP-dependent protein kinase, J. Cell Biol. 108 (1989) 2409–2422.
[30] S.-Y. Lee, E.J. Song, H.-J. Kim, H.-J. Kang, J.-H. Kim, K.-J. Lee, Rac1 regulates heat shock responses by reorganization of vimentin filaments: identification using MALDI-TOF MS, Cell Death Differ. 8 (2001) 1093–1102.
[31] B. Maro, M. Bornens, Reorganization of HeLa cell cytoskeleton induced by an uncoupler of oxidative phosphorylation, Nature 295 (1982) 334–336.
[32] M. Matsuyama, H. Tanaka, A. Inoko, H. Goto, S. Yonemura, K. Kobori, Y. Hayashi, E. Kondo, S. Itohara, I. Izawa, M. Inagaki, Defect of mitotic vimentin phosphorylation causes microophthalmia and cataract via aneuploidy and senescence in lens epithelial cells, J. Biol. Chem. 288 (2013) 35626–35635.
[33] A. Mónico, E. Rodríguez-Senra, F.J. Cañada, S. Zorrilla, D. Pérez-Sala, Drawbacks of dialysis procedures for removal of EDTA, PLoS One 12 (2017) e0169843.
[34] M. Nassar, H. Samaha, M. Ghabriel, M. Yehia, H. Taha, S. Salem, K. Shaaban, M. Omar, N. Ahmed, S. El-Naggar, LC3A silencing hinders aggresome vimentin cage clearance in primary choroid plexus carcinoma, Sci. Rep. 7 (2017) 8022.
[35] B. Noding, H. Herrmann, S. Koster, Direct observation of subunit exchange along mature vimentin intermediate filaments, Biophys. J. 107 (2014) 2923–2931.
[36] C.L. Oeste, B. Díez-Dacal, F. Bray, M. García de Lacoba, B.G. de la Torre, D. Andreu, A.J. Ruiz-Sánchez, E. Pérez-Inestrosa, C.A. García-Domínguez, J.M. Rojas, D. Pérez-Sala, The C-terminus of H-Ras as a target for the covalent binding of reactive compounds modulating Ras-dependent pathways, PLoS One 6 (2011) e15866.
[37] M.B. Omary, N.O. Ku, G.Z. Tao, D.M. Toivola, J. Liao, "Heads and tails" of intermediate filament phosphorylation: multiple sites and functional insights, Trends Biochem. Sci. 31 (2006) 383–394.
[38] C. Ospelt, H. Bang, E. Feist, G. Camici, S. Keller, J. Detert, A. Kramer, S. Gay, K. Ghannam, G.R. Burmester, Carbamylation of vimentin is inducible by smoking and represents an independent autoantigen in rheumatoid arthritis, Ann. Rheum. Dis. 76 (2017) 1176–1183.
[39] Z.K. Papanyan, Interaction of L-cysteine with dimethyl sulfoxide in mild conditions, Proc. Yerevan State Univ. 2 (2013) 11–14.
[40] S. Patergnani, F. Baldassari, E. De Marchi, A. Karkucinska-Wieckowska, M.R. Wieckowski, P. Pinton, Methods to monitor and compare mitochondrial and glycolytic ATP production, Methods Enzymol. 542 (2014) 313–332.
[41] V. Pekovic, I. Gibbs-Seymour, E. Markiewicz, F. Alzoghaibi, A.M. Benham, R. Edwards, M. Wenhert, T. von Zglinicki, C.J. Hutchison, Conserved cysteine residues in the mammalian lamin A tail are essential for cellular responses to ROS generation, Aging Cell 10 (2011) 1067–1079.
[42] D. Pérez-Sala, C.L. Oeste, A.E. Martínez, B. Garzón, M.J. Carrasco, F.J. Cañada, Vimentin filament organization and stress sensing depend on its single cysteine residue and zinc binding, Nat. Commun. 6 (2015) 7287.
[43] R.A. Quinlan, W.W. Franke, Molecular interactions in intermediate-sized filaments revealed by chemical cross-linking, Eur. J. Biochem. 132 (1983) 477–484.
[44] L.S. Rathje, N. Nordgren, T. Pettersson, D. Ronnlund, J. Widengren, P. Aspenstrom, A.K. Gad, Oncogenes induce a vimentin filament collapse mediated by HDAC6 that is linked to cell stiffness, Proc. Natl. Acad. Sci. USA 111 (2014) 1515–1520.
[45] A. Robert, H. Herrmann, M.W. Davidson, V.I. Gelfand, Microtubule-dependent transport of vimentin filament precursors is regulated by actin and by the concerted action of Rho- and p21-activated kinases, FASEB J. 28 (2014) 2879–2890.
[46] A. Robert, M.J. Rossow, C. Hookway, S.A. Adam, V.I. Gelfand, Vimentin filament precursors exchange subunits in an ATP-dependent manner, Proc. Natl. Acad. Sci. USA 112 (2015) E3505–E3514.
[47] K.R. Rogers, H. Herrmann, W.W. Franke, Characterization of disulfide crosslink formation of human vimentin at the dimer, tetramer, and intermediate filament levels, J. Struct. Biol. 117 (1996) 55–69.
[48] F. Rusnak, T. Reiter, Sensing electrons: protein phosphatase redox regulation, Trends Biochem. Sci. 25 (2000) 527–529.
[49] F.J. Sánchez-Gómez, E. Cernuda-Morollón, K. Stamatakis, D. Pérez-Sala, Protein thiol modification by 15-deoxy-$\Delta^{12,14}$-prostaglandin J_2 addition in mesangial cells: role in the inhibition of pro-inflammatory genes, Mol. Pharmacol. 66 (2004) 1349–1358.
[50] R.L. Shoeman, B. Honer, T.J. Stoller, C. Kesselmeier, M.C. Miedel, P. Traub, M.C. Graves, Human immunodeficiency virus type 1 protease cleaves the intermediate filament proteins vimentin, desmin, and glial fibrillary acidic protein, Proc. Natl. Acad. Sci. USA 87 (1990) 6336–6340.
[51] R.K. Sihag, M. Inagaki, T. Yamaguchi, T.B. Shea, H.C. Pant, Role of phosphorylation on the structural dynamics and function of types III and IV intermediate filaments, Exp. Cell Res. 313 (2007) 2098–2109.
[52] A.V. Sokolova, L. Kreplak, T. Wedig, N. Mucke, D.I. Svergun, H. Herrmann, U. Aebi, S.V. Strelkov, Monitoring intermediate filament assembly by small-angle x-ray scattering reveals the molecular architecture of assembly intermediates, Proc. Natl. Acad. Sci. USA 103 (2006) 16206–16211.
[53] K. Stamatakis, D. Pérez-Sala, Prostanoids with cyclopentenone structure as tools for the characterization of electrophilic eicosanoid-protein interactomes, Ann. N. Y. Acad. Sci. 1091 (2006) 548–570.
[54] K. Stamatakis, F.J. Sánchez-Gómez, D. Pérez-Sala, Identification of novel protein targets for modification by 15-deoxy-$D^{12,14}$-prostaglandin J_2 in mesangial cells reveals multiple interactions with the cytoskeleton, J. Am. Soc. Nephrol. 17 (2006) 89–98.
[55] J.N. Stannard, B.L. Horecker, The in vitro inhibition of cytochrome oxidase by azide and cyanide, J. Biol. Chem. 172 (1948) 599–608.
[56] D.M. Toivola, P. Strnad, A. Habtezion, M.B. Omary, Intermediate filaments take the heat as stress proteins, Trends Cell Biol. 20 (2010) 79–91.
[57] P. Traub, C.E. Vorgias, Involvement of the N-terminal polypeptide of vimentin in the formation of intermediate filaments, J. Cell Sci. 63 (1983) 43–67.
[58] K. Uchida, L.I. Szweda, H.Z. Chae, E.R. Stadtman, Immunochemical detection of 4-hydroxynonenal protein adducts in oxidized hepatocytes, Proc. Natl. Acad. Sci. USA 90 (1993) 8742–8746.
[59] P. Vallotton, S. Olivier, Tri-track: free software for large scale particle tracking, Microsc. Microanal. 19 (2013) 451–460.
[60] Á. Viedma-Poyatos, Y.d. Pablo, M. Pekny, D. Pérez-Sala, The cysteine residue of glial fibrillary acidic protein is a critical target for lipoxidation and required for efficient network organization, Free Rad. Biol. Med. 120 (2018) 380–394.
[61] K.L. Vikstrom, S.S. Lim, R.D. Goldman, G.G. Borisy, Steady state dynamics of intermediate filament networks, J. Cell Biol. 118 (1992) 121–129.
[62] G. Vistoli, D. De Maddis, A. Cipak, N. Zarkovic, M. Carini, G. Aldini, Advanced glycoxidation and lipoxidation end products (AGEs and ALEs): an overview of their mechanisms of formation, Free Radic. Res. 47 (2013) 3–27.
[63] S. Winheim, A.R. Hieb, M. Silbermann, E.M. Surmann, T. Wedig, H. Herrmann, J. Langowski, N. Mucke, Deconstructing the late phase of vimentin assembly by total internal reflection fluorescence microscopy (TIRFM), PLoS One 6 (2011) e19202.
[64] S. Yamaguchi, G. Aldini, S. Ito, N. Morishita, T. Shibata, G. Vistoli, M. Carini, K. Uchida, Delta(12)-prostaglandin J(2) as a product and ligand of human serum albumin: formation of an unusual covalent adduct at His146, J. Am. Chem. Soc. 132 (2010) 824–832.
[65] T. Yamaguchi, H. Goto, T. Yokoyama, H. Sillje, A. Hanisch, A. Uldschmid, Y. Takai, T. Oguri, E.A. Nigg, M. Inagaki, Phosphorylation by Cdk1 induces Plk1-mediated vimentin phosphorylation during mitosis, J. Cell Biol. 171 (2005) 431–436.
[66] M. Yoon, R.D. Moir, V. Prahlad, R. Goldman, Motile properties of vimentin intermediate filament networks in living cells, J. Cell Biol. 143 (1998) 147–157.